

Synthesis, Properties, and Redox Behavior of Tetracyanobutadiene and Dicyanoquinodimethane Chromophores Bearing Two Azulenyl Substituents

Taku Shoji,^{*,†} Mitsuhsa Maruyama,[†] Erika Shimomura,[†] Akifumi Maruyama,[†] Shunji Ito,[‡] Tetsuo Okujima,[§] Kozo Toyota,^{||} and Noboru Morita^{||}

[†]Department of Chemistry, Faculty School of Science, Shinshu University, Matsumoto 390-8621, Japan

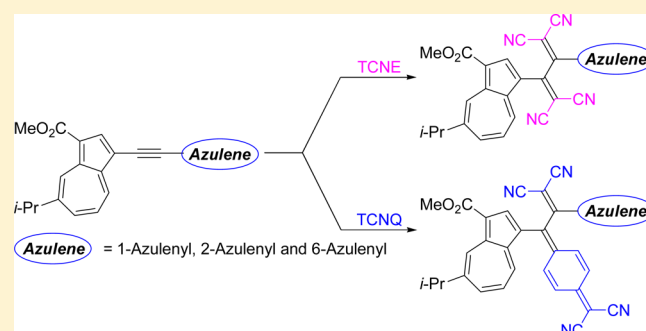
[‡]Graduate School of Science and Technology, Hirosaki University, Hirosaki 036-8561, Japan

[§]Department of Chemistry and Biology, Graduate School of Science and Engineering, Ehime University, Matsuyama 790-8577, Japan

^{||}Department of Chemistry, Graduate School of Science, Tohoku University, Sendai 980-8578, Japan

S Supporting Information

ABSTRACT: Acetylene derivatives with an azulenyl group at both terminals have been prepared by palladium-catalyzed alkylation under Sonogashira–Hagihara conditions. These alkynes reacted with tetracyanoethylene and 7,7,8,8-tetracyanoquinodimethane in a formal [2 + 2] cycloaddition–retroelectrocyclization reaction to afford the corresponding new tetracyanobutadienes (TCBDs) and dicyanoquinodimethanes (DCNQs), respectively, in excellent yields. Intramolecular CT absorption bands were found in the UV–vis spectra of the novel chromophores, and CV and DPV showed that they exhibited a reversible two-stage reduction wave, due to the electrochemical reduction of TCBD and DCNQ moieties. Color changes were also observed during the electrochemical reduction.



INTRODUCTION

Organic donor–acceptor systems featuring intramolecular charge-transfer (ICT) interactions have attracted considerable interest as promising candidates for the next generation of organic electronic and optoelectronic devices.¹ As one way to construct the donor–acceptor (D–A) systems, Diederich and Michinobu utilized the click-reaction, which involved a formal [2 + 2] cycloaddition–retroelectrocyclization process, of electron-rich alkynes with tetracyanoethylene (TCNE),² 7,7,8,8-tetracyanoquinodimethane (TCNQ),³ dicyanovinyl and tricyanovinyl derivatives.⁴ They also reported that novel D–A systems obtained by these reactions could be applied to advanced materials, such as third-order nonlinearity materials and metal-ion sensors.

Azulene has attracted the interest of many research groups due to its unusual properties associated with its remarkable polarizability as well as its beautiful blue color.⁵ The azulene system also has a tendency to stabilize both cations and anions, depending on the substitution position, through the contributions of its formal tropylium and cyclopentadienide substructures. Thus, the substitution by azulenyl group via its 1- and 3-positions promotes extreme electron-donating nature, while azulene-4-yl, -6-yl, and -8-yl substituents are also strongly electron-withdrawing characters. Amphoteric properties are expected by the substitution at the 2-position of the azulene

ring. We have prepared novel π -electron systems with a variety of 2-azulenyl or 6-azulenyl substituents for the creation of multistage redox systems by utilizing the electronic properties of the azulene substituents.⁶ The azulene-substituted π -electron systems also exhibit a significant color change by electrochemical reactions. Recently, we have reported the [2 + 2] cycloaddition–retroelectrocyclization reactions of several 1-ethynylazulene derivatives with TCNE and/or TCNQ by utilizing the strong electron-donating nature of the group to give the corresponding tetracyanobutadienes (TCBDs) and dicyanoquinodimethanes (DCNQs), which displayed intramolecular charge-transfer (ICT) characters.⁷ We revealed their multistep reduction behavior by using cyclic voltammetry (CV) and differential pulse voltammetry (DPV). Moreover, significant color changes were observed by the electrochemical reduction of the new chromophores, although improvement of the redox stability toward the electrochemical reaction remained as a subject for the device application. The TCBD and DCNQ derivatives with both 1-azulenyl and 2-azulenyl or 6-azulenyl groups should have more stable redox cycles and improved electrochromic properties, over TCBDs and DCNQs substituted by the same two 1-azulenyl groups, because 2-

Received: October 4, 2013

Published: December 4, 2013

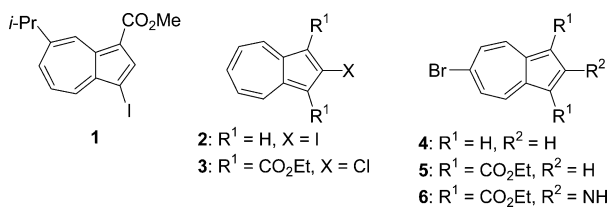
azulenyl and 6-azulenyl groups tend to stabilize an anionic species by the contribution of their resonance structures. However, the TCBD and DCNQ derivatives bearing two azulene groups substituted at different positions on azulene ring (i.e., 1-azulenyl with 2-azulenyl or 6-azulenyl groups) have not yet been explored. In this research these positional differences in the substitution positions of the azulene ring are applied to further understanding of the TCBD and DCNQ derivatives. These investigations could be favorably carried out with using the azulene derivatives.

Herein, we describe the synthesis of diazulenylacetylene derivatives under Sonogashira–Hagihara reaction conditions as well as the reactivity of the products toward the [2 + 2] cycloaddition reaction with TCNE and TCNQ to afford the corresponding TCBD and DCNQ chromophores possessing two azulenyl groups. The electronic properties of the novel TCBD and DCNQ derivatives are characterized by electrochemical analysis and absorption spectroscopy.

RESULTS AND DISCUSSION

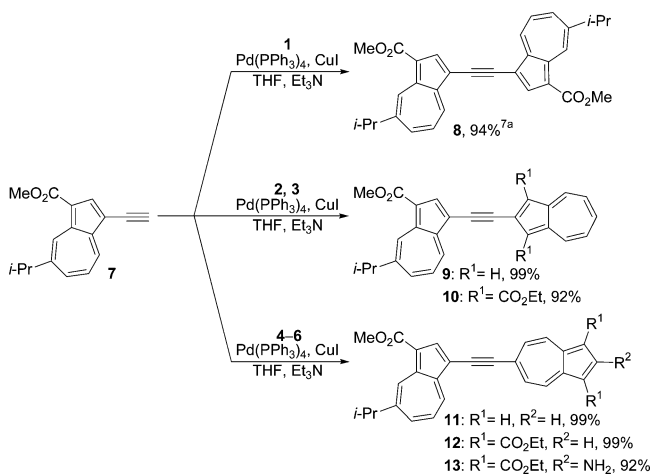
Synthesis of Diazulenylacetylenes. Preparation of diazulenylacetylenes 8–13 was required to construct the novel TCBD and DCNQ derivatives with two azulene substituents. Di(1-azulenyl)acetylene 8 had been previously prepared in 94% yield.^{7a} Thus, the diazulenylacetylenes 9–13 were prepared by the palladium-catalyzed alkynylation of 1-ethynylazulene 7 with the corresponding haloazulenes 1–6 (Chart 1) under the Sonogashira–Hagihara conditions

Chart 1. Structures of 1-Halo-, 2-Halo- and 6-Haloazulenes 1–6



(Scheme 1). As in the preparation of 8, (1-azulenyl)(2-azulenyl)acetylene 9 was obtained in 99% yield by the cross-coupling reaction of 7 with 2-iodoazulene (2)⁸ in the presence of Pd(PPh₃)₄ as a catalyst in THF/Et₃N at 50 °C. The reaction

Scheme 1. Synthesis of Diazulenylacetylenes 8–13

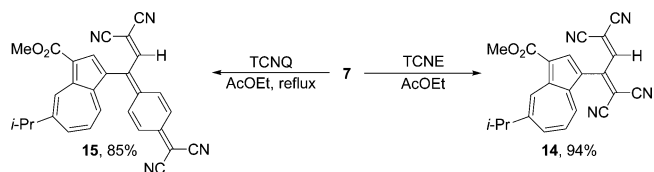


of diethyl 2-chloroazulene-1,3-dicarboxylate (3)⁹ with 7 under similar reaction conditions afforded 10 in 92% yield, although aryl chlorides are usually less reactive toward the palladium-catalyzed cross-coupling reaction than are aryl iodides and bromides.¹⁰ High yield of the product 10 was attributable to both the high reactivity of 1-ethynylazulene and the electron-withdrawing nature of the 1,3-bis-ethoxycarbonyl groups on the azulene ring, which should increase the reactivity toward the oxidative addition of the palladium catalyst.

The cross-coupling reaction of 6-bromoazulene (4)¹¹ with 7 in the presence of the palladium catalyst afforded (1-azulenyl)(6-azulenyl)acetylene 11 in 99% yield. Similar to the reactions described above, Sonogashira–Hagihara reaction of 7 with 6-bromoazulene derivatives 5 and 6¹² gave the corresponding cross-coupled products 12 and 13 in 99 and 92% yields, respectively. The new diazulenylacetylene derivatives 9–13 along with di(1-azulenyl)acetylene 8 possess fair solubility in general organic solvents, such as chloroform and dichloromethane. Moreover, they are stable and show no decomposition even after several weeks at room temperature. Thus, the diazulenylacetylenes 8–13 could be utilized in further transformations for the synthesis of new TCBD and DCNQ derivatives bearing two azulene substituents because of their considerable stability and solubility, although the less stable acetylene derivatives may be utilized for the cycloaddition reaction.

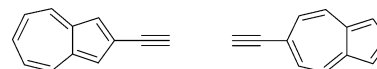
Reaction of Di(azulenyl)acetylenes with TCNE and TCNQ. We previously reported that the [2 + 2] cycloaddition reaction of 8 with TCNE proceeds smoothly to give 16 in 97% yield.^{7a} For the preparation of the reference compounds 14 and 15 in this study, the [2 + 2] cycloaddition–retroelectrocyclization sequence of 7 with TCNE and TCNQ was applied. Thus, the reaction of 7 with TCNE and TCNQ in ethyl acetate gave the corresponding TCBD 14 and DCNQ 15 in 94 and 85% yields, respectively, although the compound 7 is bearing an electron-withdrawing methoxycarbonyl group (Scheme 2). The

Scheme 2. Reaction of 7 with TCNE and TCNQ



cycloaddition reaction is required good electron-donating group on the alkyne terminal. These results indicate the strong ability of the electron-donating character of the 1-azulenyl substituent. The same reaction of 2-ethynyl¹³ and 6-ethynylazulenes¹⁴ (Chart 2) with TCNE was also examined

Chart 2. 2-Ethynyl- and 6-Ethynylazulenes

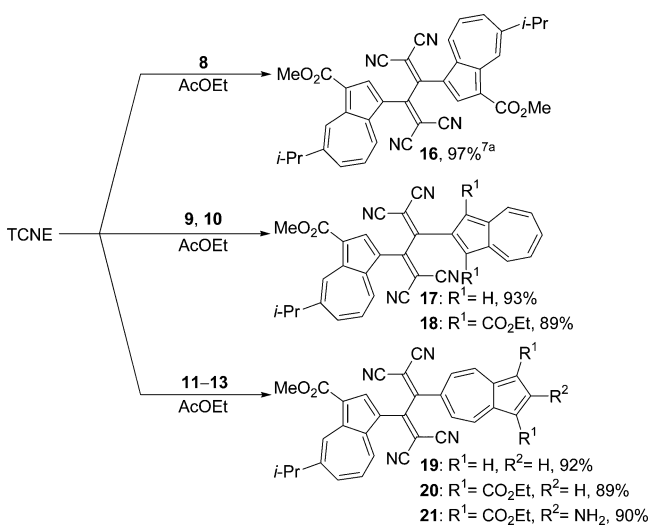


under similar reaction conditions, but the reaction did not afford the desired TCBD derivatives. The reactivity of the alkyne moiety substituted by only 2-azulenyl or 6-azulenyl group is not sufficient for the cycloaddition reaction because of their electron-withdrawing nature that is unfavorable for the cycloaddition reaction. Thus, a highly electron-donating

substituent, i.e., the 1-azulenyl group, is essential on the alkyne terminal to induce the [2 + 2] cycloaddition reaction of the acetylene derivatives with 2-ethynyl- and 6-ethynylazulene moieties.

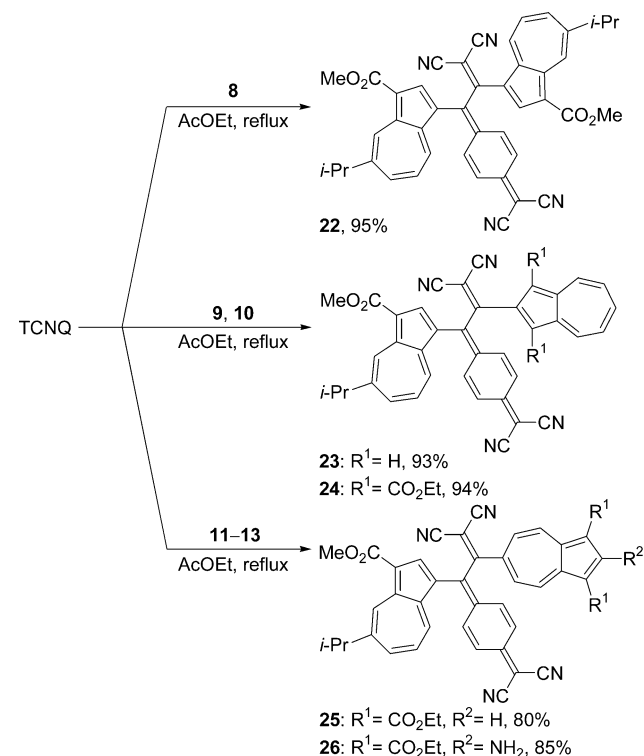
The reaction of **9**, which has both 1-azulenyl and 2-azulenyl groups, with TCNE in ethyl acetate afforded **17** in 93% yield. Alkyne derivative **10**, which possesses electron-withdrawing ethoxycarbonyl groups at the 1,3-positions on the 2-azulenyl substituent, also reacted readily with TCNE, similar to the reaction of **9**, to afford the corresponding TCBD derivative **18** in 89% yield. (1-Azulenyl)(6-azulenyl)acetylenes **11**, **12**, and **13** also reacted with TCNE in ethyl acetate to afford the corresponding [2 + 2] cycloadducts **19**, **20**, and **21** in 92, 89, and 90% yields, respectively (Scheme 3).

Scheme 3. Synthesis of Azulene-Substituted TCBDs 16–21



For the synthesis of the novel DCNQ derivatives, the [2 + 2] cycloaddition–retroelectrocyclization sequence was also applied to the reaction of acetylene derivatives **8–13** with TCNQ. The reaction of **8** with TCNQ in refluxing ethyl acetate afforded **22** in 95% yield as the sole product, although the reaction did not proceed at room temperature (Scheme 4). Previously, Diederich et al. reported that TCNQ shows lower reactivity than TCNE toward the formal [2 + 2] cycloaddition reaction with electron-rich alkynes.¹⁵ Furthermore, they reported that excess TCNQ, prolonged reaction period and elevated temperature were required to complete the reaction. Therefore, the relatively higher temperature required also reflects the lower reactivity of TCNQ than that of TCNE with azulene-substituted acetylenes. The electronically more deficient alkynes **9** and **10**, which have a 2-azulenyl substituent on the alkyne terminal, reacted with TCNQ in refluxing ethyl acetate to afford **23** and **24** in 93 and 89% yields, respectively, although a relatively longer reaction period was required. (1-Azulenyl)(6-azulenyl)acetylenes **12** and **13** also reacted with TCNQ in a similar manner, affording the corresponding [2 + 2] cycloaddition products **25** and **26** in 80 and 85% yields, respectively. The reaction of **11** in refluxing ethyl acetate gave an unidentified complex mixture instead of the desired cycloaddition product. The compound **11** was unreactive with TCNQ at room temperature. Thus, the cyclization product of **11** with TCNQ could not be obtained by the reaction.

Scheme 4. Synthesis of Azulene-Substituted DCNQs 22–26



The X-ray crystal analysis may provide direct evidence of the regiochemistry for the DCNQ moiety of the products, but the suitable single crystals for the analysis could not be obtained, so far. Thus, we have applied the complete assignment of the ¹³C NMR signals including the DCNQ moiety by utilizing 2D NMR techniques (i.e., HMQC and HMBC experiments). The observed regiochemistry is in consistent with the previous results that the DCNQ moiety is located to the side of electron-donating group.

Spectroscopic Properties. The new compounds **9–15** and **17–26** were fully characterized spectroscopically. ESI and FAB mass spectra of **9–15** and **17–26** showed the correct molecular ion peaks observed as [M + Na]⁺ and [M]⁺ ion peaks, respectively. The characteristic stretching vibration band of the C≡N moieties of **14**, **15**, and **17–26** was observed at $\nu_{\max} = 2206\text{--}2230\text{ cm}^{-1}$ in the IR spectra, instead of the characteristic stretching band for the C≡C triple bond of the starting acetylene derivatives. Assignment of the peaks in the ¹H and ¹³C NMR spectra of the compounds was accomplished by COSY, HMQC, and HMBC experiments. These results are consistent with the structure of these products. The ¹H NMR spectra of alkyne **7**, TCBD **14**, and DCNQ **15** in CDCl₃ are shown in Figure 1. Significant downfield shifts for seven-membered ring protons (4-H, 6-H, and 7-H) of the azulene moiety of TCBD **14** and DCNQ **15** were observed in CDCl₃ compared with that of **7**, which is attributable to the resonance effect with the strong electron-withdrawing TCBD and DCNQ groups as illustrated in Scheme 5. The upfield shift for proton 8-H of **14** and **15** is attributed to the anisotropic effect of the adjacent cyano groups.¹⁶

UV–vis spectra of TCBDs **19–21** in dichloromethane and DCNQ **22** in CH₂Cl₂/hexane in several proportions are shown in Figures 2 and 3, respectively. The absorption maxima (λ_{\max}) and their coefficients (log ϵ) of the new compounds **9–15** and

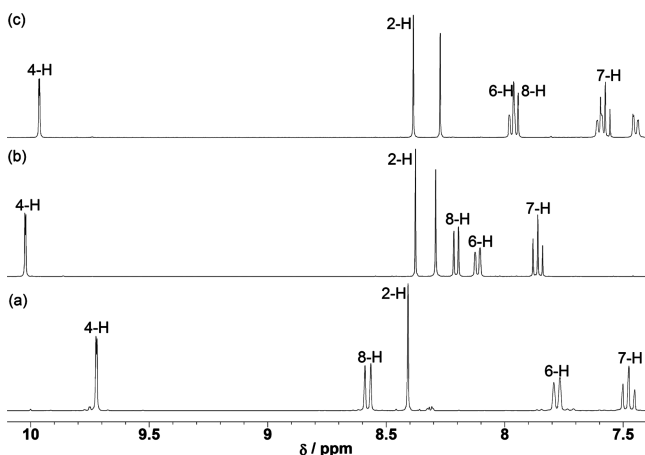


Figure 1. ^1H NMR spectra (500 MHz) of (a) **7**, (b) **14**, and (c) **15** in CDCl_3 .

Scheme 5. Plausible Resonance Structures of **14** and **15**

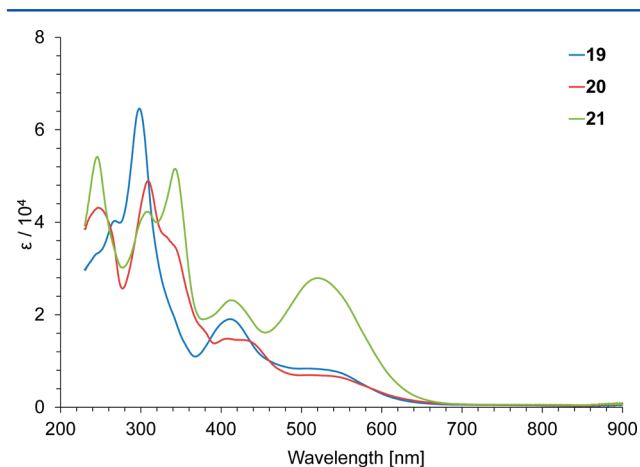
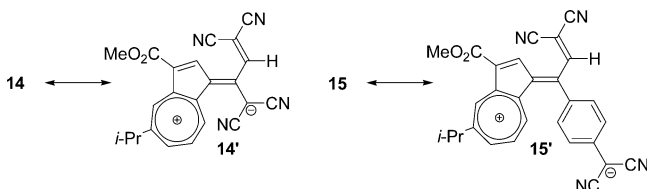


Figure 2. UV-vis spectra of **19** (blue line), **20** (red line), and **21** (green line) in dichloromethane.

17–26 are summarized in the Experimental Section. The UV-vis spectra of the new acetylene derivatives **9–13** showed characteristic weak absorptions arising from the azulene system in the visible region (see the Supporting Information). Compounds **9–13** also exhibited relatively strong absorptions around 450 nm, which may be attributable to intramolecular charge transfer (ICT) between the two azulene rings through the $\text{C}\equiv\text{C}$ triple bond, because these bands could not be observed in the spectrum of 1-ethynylazulene **7**.

To examine the theoretical aspects of the spectroscopic properties depending on the substitution position of these series, molecular orbital calculations were performed on **9** and **11** as model compounds, which do not exhibit conformational isomerism, using B3LYP/6-31G** density functional theory.¹⁷ The frontier Kohn–Sham orbitals of **9** and **11** are shown in the Supporting Information. Judging from the comparison between

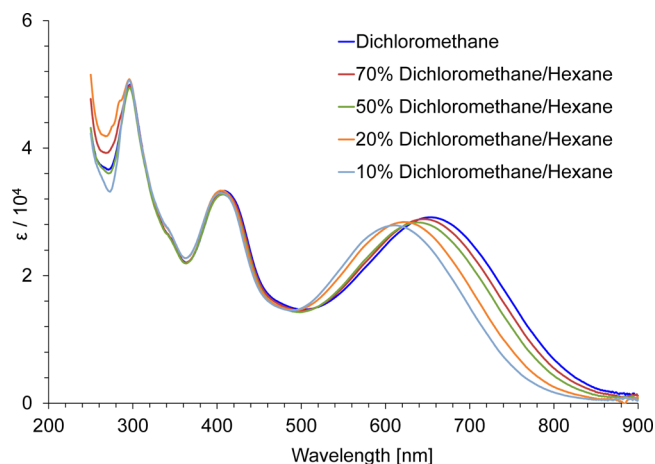


Figure 3. Solvent dependence of the UV-vis spectrum of **22** in dichloromethane/hexane.

the experimental and the theoretical UV-vis spectra, the absorption maxima of **9** and **11** were assignable to overlaps of some transitions as shown in Table 1. The strong absorption

Table 1. Electronic Transitions Derived from the Computed Values Based on B3LYP/6-31G** Method and Experimental Values of **9** and **11**

| sample | experimental λ_{max} ($\log \epsilon$) | computed value λ_{max} (strength) | composition of band ^a /CI coefficients ^b |
|-----------|---|--|--|
| 9 | 573 (3.17) | 582 (0.0071) | H \rightarrow L (0.9413) |
| | | | H \rightarrow L+1 (−0.2489) |
| | 457 (4.59) | 439 (1.1440) | H \rightarrow L (0.2292) |
| | | H \rightarrow L+1 (0.9324) | |
| 11 | 568 (3.15) | 568 (0.0067) | H−1 \rightarrow L (0.9496) |
| | | 552 (0.0089) | H \rightarrow L (0.2571) |
| | | | H \rightarrow L+1 (0.9073) |
| | | | H \rightarrow L+2 (−0.2360) |
| | 454 (4.72) | 422 (1.2562) | H−1 \rightarrow L+1 (0.9480) |
| | 430 sh (4.66) | 404 (0.0003) | H \rightarrow L+1 (0.2607) |
| | | H \rightarrow L+2 (0.9587) | |

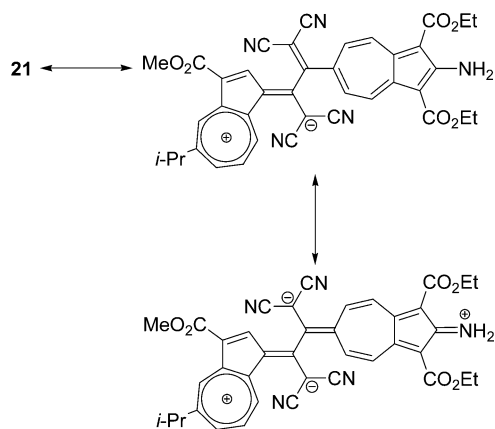
^aH = HOMO; L = LUMO. ^bCI = configuration interaction.

bands at $\lambda_{\text{max}} = 457$ nm and $\lambda_{\text{max}} = 435$ nm of **9** were considered to be the transition from the HOMO located on the 2-azulenyl group to the LUMO+1 located on the 1-azulenyl group with the electron-withdrawing methoxycarbonyl substituent. The calculations also revealed that the ICT contribution of **9** from the 1-azulenyl to the 2-azulenyl group (HOMO \rightarrow LUMO) was relatively small (Table 1). Thus, the absorption band could be assigned to the ICT from the 2-azulenyl to 1-azulenyl groups. The ICT of **11** confirmed that the absorption band at $\lambda_{\text{max}} = 454$ nm arose from the HOMO−1 \rightarrow LUMO+1, which corresponds to the transition from the 6-azulenyl to the 1-azulenyl group. The calculation also displayed the contribution from the transition from the 1-azulenyl to 6-azulenyl groups (HOMO \rightarrow LUMO+1 and HOMO \rightarrow LUMO+2), although it was relatively low. The weak longest wavelength absorption bands of **9** ($\lambda_{\text{max}} = 573$ nm) and **11** ($\lambda_{\text{max}} = 568$ nm) were confirmed to arise from the overlap of the π – π^* transitions of the substituted azulene rings themselves.

The UV-vis spectrum of the simpler TCBD derivative **14** showed an absorption in the visible region at $\lambda_{\text{max}} = 560$ nm.

The extinction coefficient for the longest wavelength absorption band of **14** was a quarter that of **16**. These results suggest that ICT character from the two azulene rings is effectively employed by the cross-conjugated TCBD ring. The TCBD derivative with a 2-azulenyl substituent **17** exhibited an absorption band at $\lambda_{\max} = 410$ nm, which extended beyond 700 nm, in the visible region. The longest wavelength absorption maximum of TCBD **18** ($\lambda_{\max} = 558$ nm) in dichloromethane showed a bathochromic shift relative to that of **17** in the same solvent. These effects indicate a lower HOMO–LUMO gap of **18**, compared to that of **17**, due to the electron-withdrawing 1,3-bisethoxycarbonyl groups on the 2-azulenyl substituent. Although the longest wavelength absorption maxima of **19** [$\lambda_{\max} = 545$ (sh) nm] and **20** [$\lambda_{\max} = 558$ (sh) nm] showed small absorption coefficients at almost the same value, a relatively strong absorption band in the visible region was observed in **21** ($\lambda_{\max} = 510$ nm) as shown in Figure 2. These results are ascribed to the quinoid form of the 6-azulenyl moiety by the resonance with the 2-amino moiety of **21** (Scheme 6).

Scheme 6. Plausible Resonance Structures of **21**



Most of the DCNQ chromophores showed intense ICT absorption bands, which depended on the polarity of the solvent, in the visible region. The absorption band of **22** at $\lambda_{\max} = 655$ nm in dichloromethane exhibited a large blue shift of 44 nm in the less polar 10% CH_2Cl_2 /hexane, which suggests the ICT nature of this band (Figure 3).¹⁸ Similar to **22**, DCNQs **23** and **24** with a 2-azulenyl substituent showed a broad ICT absorption band centered at $\lambda_{\max} = 631$ nm and $\lambda_{\max} = 721$ nm in dichloromethane, respectively. In these cases, the longest wavelength absorption maxima also exhibited hypsochromic shifts in 10% CH_2Cl_2 /hexane (**23** $\lambda_{\max} = 592$ nm and **24** $\lambda_{\max} = 670$ nm). The shift value of **23** (39 nm) and **24** (51 nm) is larger than those of the corresponding TCBDs **17** (9 nm) and **18** (1 nm) under the same conditions. These results indicate that the first excited state has a larger dipole moment compared to that in the ground state, because of the effective ICT character from azulene to the DCNQ unit. A broad absorption centered at $\lambda_{\max} = 647$ nm that extended beyond $\lambda_{\max} = 900$ nm was also observed in **25** in dichloromethane. The UV–vis spectrum of **26** also displayed a broad absorption at $\lambda_{\max} = 644$ nm in dichloromethane. When the solvent was changed to the less polar 10% CH_2Cl_2 /hexane, the longest wavelength absorption band of **25** and **26** showed an apparent blue-shift to $\lambda_{\max} = 597$ nm and $\lambda_{\max} = 586$ nm, respectively.

Electrochemistry. To clarify the effect on the electrochemical properties of substitution positions on the azulene ring in TCBD and DCNQ derivatives that include two azulenyl groups, the redox behavior of the novel chromophores **14**, **15**, and **17–26** was examined by CV and DPV. Measurements were carried out with a standard three-electrode configuration. Tetraethylammonium perchlorate (0.1 M) in benzonitrile was used as a supporting electrolyte, with a platinum wire auxiliary and disk working electrodes. All measurements were carried out under an argon atmosphere, and the potentials were related to a standard Ag/AgNO₃ reference electrode. The half-wave potential of the ferrocene–ferrocenium ion couple (Fc/Fc⁺) under these conditions using this reference electrode was observed at +0.15 V during CV. The accuracy of the reference electrode was confirmed by CV measurements of the couple in each sample as an internal ferrocene standard. The redox potentials (in volts vs Ag/AgNO₃) of **14**, **15**, and **17–26** measured under a scan rate of 100 mV s⁻¹ are summarized in Table 2.

Table 2. Redox Potentials^{a,b} of the ICT Chromophores **14**, **15**, and **17–26** and TCBDs **16** and **27**^{7a} and DCNQ **28**^{7b} as Reference Compounds

| sample | method | E_1^{red} [V] | E_2^{red} [V] | E_3^{red} [V] |
|-------------------------|--------|------------------------|------------------------|------------------------|
| 14 | CV | – | – | – |
| | (DPV) | (–0.43) | (–1.05) | (–1.82) |
| 15 | CV | –0.31 | –0.62 | |
| | (DPV) | (–0.29) | (–0.60) | (–1.94) |
| 16 ^{7a} | CV | –0.64 | –1.04 | |
| | (DPV) | (–0.62) | (–1.02) | (–1.92) |
| 17 | CV | –0.64 | –0.96 | |
| | (DPV) | (–0.62) | (–0.94) | (–1.84) |
| 18 | CV | –0.50 | –0.98 | |
| | (DPV) | (–0.48) | (–0.96) | (–1.80) |
| 19 | CV | –0.50 | –0.90 | |
| | (DPV) | (–0.48) | (–0.88) | (–1.80) |
| 20 | CV | –0.40 | –0.76 | |
| | (DPV) | (–0.38) | (–0.74) | (–1.63) |
| 21 | CV | –0.53 | –0.92 | |
| | (DPV) | (–0.51) | (–0.90) | (–1.81) |
| 22 | CV | –0.47 | –0.62 | |
| | (DPV) | (–0.45) | (–0.60) | (–1.84) |
| 23 | CV | –0.49 | –0.60 | |
| | (DPV) | (–0.47) | (–0.58) | (–1.91) |
| 24 | CV | –0.34 | –0.59 | |
| | (DPV) | (–0.32) | (–0.57) | (–1.66) |
| 25 | CV | –0.33 | –0.48 | |
| | (DPV) | (–0.31) | (–0.46) | (–1.56) |
| 26 | CV | –0.38 | –0.53 | |
| | (DPV) | (–0.36) | (–0.51) | (–1.82) |
| 27 ^{7a} | CV | –0.61 | –1.03 | |
| | (DPV) | (–0.59) | (–1.01) | (–1.95) |
| 28 ^{7b} | CV | –0.43 | –0.59 | |
| | (DPV) | (–0.41) | (–0.58) | (–0.90) |

^aV vs Ag/AgNO₃, 1 mM in benzonitrile containing Et₄NClO₄ (0.1 M), Pt electrode (internal diameter: 1.6 mm), scan rate = 100 mV s⁻¹ and internal reference (Fc/Fc⁺ = +0.15 V). In the cases of reversible waves, redox potentials measured by CV are presented. The peak potentials measured by DPV are shown in parentheses. ^bHalf-wave potentials $E^{\text{red}} = (E_{\text{pc}} + E_{\text{pa}})/2$ on CV, E_{pc} and E_{pa} correspond to the cathodic and anodic peak potentials, respectively.

TCBD chromophores possessing two azulenyl substituents **16**–**21** showed reversible two-stage reduction waves during CV due to the reduction of the TCBD unit, although TCBD **14** did not exhibit a reversibility in the reduction waves. Thus, two azulenyl groups on the TCBD unit are essential for stabilizing the anionic species generated by the electrochemical reduction. TCBD **17** displayed a reversible two-step reduction wave. The potentials were identified by CV as -0.64 and -0.96 V, to generate up to a dianionic species. The electrochemical reduction of **18** also exhibited a reversible two-step wave at -0.50 and -0.98 V during CV. A positive shift of the first reduction potential of **17** compared with that of **18** is attributable to the decrement of the LUMO-level due to the electron-withdrawing nature of the two ethoxycarbonyl groups at the 1,3-positions. Reversible redox waves were also observed by the electrochemical reduction of TCBDs **19**, **20**, and **21** substituted by a 6-azulenyl group, which could be ascribed to the formation of a dianionic species. TCBD derivative **19** with a 6-azulenyl substituent exhibited a reversible two-step reduction wave with potentials at -0.50 and -0.90 V. The first reduction potential of **19** showed a positive shift compared with that of **17**, which was attributable to the higher electron affinity of the 6-azulenyl group than that of the 2-azulenyl group. In the case of the electrochemical analysis of **20**, a reversible two-step reduction wave (-0.40 and -0.76 V) was observed by CV, because of the redox activities of the TCBD unit. The first reduction potential of **20** showed a positive shift compared with **19**, similar to TCBDs with a 2-azulenyl substituent. The electrochemical reduction of **21** also showed a reversible two-step reduction wave during CV (-0.53 and -0.92 V) due to stepwise formation up to a dianionic species. Despite the existence of electron-withdrawing ethoxycarbonyl groups at the 1,3-positions, the first reduction potential of **21** exhibited the most negative value among TCBDs with a 6-azulenyl group **19**, **20**, and **21**. Thus, it is concluded that the 2-amino moiety of **21** increased the LUMO-level by its electron-donating nature.

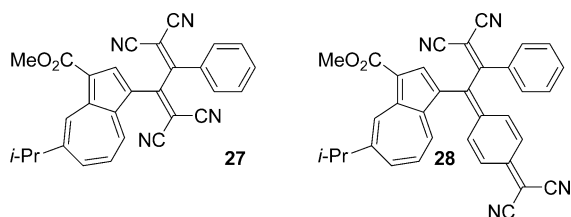
DCNQ **22** with two azulene moieties exhibited a reversible two-step wave, the potentials of which were identified at -0.47 and -0.62 V by CV as half-wave potentials, because of the formation of a radical anionic and a dianionic species, respectively. As shown in Table 2, electrochemical reduction of DCNQs **23**–**26** also showed a reversible two-stage reduction wave during CV, which could be attributed to the stepwise formation to a dianionic species. DCNQs **23**–**26** exhibited less negative reduction potentials compared with those of the corresponding TCBD chromophores. These results are ascribed to the higher electron-accepting nature of the DCNQ moiety than that of the corresponding TCBD unit. We have previously reported the redox properties of TCBD and DCNQ derivatives with both 1-azulenyl and phenyl substituents **27** and **28** (Chart 3). These compounds exhibited

the first reduction potentials at -0.61 and -0.43 V, respectively. The TCBDs with a 6-azulenyl group **19**–**21** and DCNQs **25** and **26** displayed less negative reduction potentials compared with those of **27** and **28**. According to these results, the 6-azulenyl moiety possesses a higher electron affinity than that of the phenyl substituent with respect to the reduction potentials observed by CV.

Electrochromism is observed in reversible redox systems that exhibit significant color changes in their different oxidation states. Stabilization of the redox cycle is very important in the construction of electrochromic materials, because the molecules used for these applications require high redox stabilities. Recently, we developed various azulene-substituted, redox-active chromophores with the aim of creating stabilized electrochromic materials.¹⁹ As part of the study, we reported several TCBD derivatives bearing 1-azulenyl substituents, in which we identified some novel hybrid structures of violen and cyanine with redox activities. From our previous study, 2-azulenyl or 6-azulenyl groups connected by π -electron systems induced electrochromic properties with high reversibility. Specifically, electrochromic properties of TCBD derivatives substituted by both ferrocenyl and 2-azulenyl or 6-azulenyl groups exhibited color changes with higher reversibility, attributable to the stabilization of anionic species during the electrochemical reaction.^{7e} However, the electrochromic properties of DCNQ derivatives substituted by a 2-azulenyl or 6-azulenyl group have not yet been explored. DCNQs with a 2-azulenyl or 6-azulenyl moiety might exemplify a new class of electrochromic materials. Thus, the visible spectra of TCBDs **17**–**21** and DCNQs **22**–**26** were monitored to identify color changes that occurred during the electrochemical reactions. Constant-current oxidation and reduction (100 mA) was applied to the solutions of **17**–**26** with a platinum mesh as the working electrode and a wire counter electrode in an electrolytic cell of 1 mm thickness. Visible spectra were measured in degassed benzonitrile containing Et_4NClO_4 (0.1 M) as the supporting electrolyte at room temperature under electrochemical reaction conditions.

When the spectral changes of **17** were monitored during the electrochemical reduction, the absorption in the visible region gradually increased with the development of new absorptions at $\lambda_{\text{max}} = 550$ nm and $\lambda_{\text{max}} = 710$ nm, which reached the near-infrared region. The color change should be attributable to the formation of an anionic species formed by the electrochemical reduction of **17**. However, reverse oxidation of the reduced species of **17** did not regenerate the spectrum of the parent **17**, although good reversibility was observed in the two-step reduction by CV. The poor reversibility of the color changes was attributable to the instability of the dianionic species produced by the two-electron reduction. When the UV–vis spectrum of **18** was measured under electrochemical reduction conditions, the absorption bands of **18** in the visible region gradually increased with the appearance of new absorption bands that reached the near-infrared region. In contrast to the results of **17**, reverse oxidation regenerated the original absorption bands of **18**. The good reversibility for the redox process of **18** indicates the generation of a stabilized anionic species probably due to the substitution by the electron-withdrawing ethoxycarbonyl group at the 1,3-positions on the 2-azulenyl group. Visible spectra of **19** were measured under electrochemical reduction conditions, and the absorption band in the near-infrared region gradually increased along with a color change from red to blue. Reverse oxidation of the reduced

Chart 3. TCBD **27** and DCNQ **28** with 1-Azulenyl and Phenyl Substituents



species regenerated the original color of **19**. Similarly, an absorption band in the near-infrared region gradually developed by the electrochemical reduction of **20**. Reverse oxidation of the reduced species decreased the new absorption bands, along with recovery of the parent color of **20** (Figure 4). The

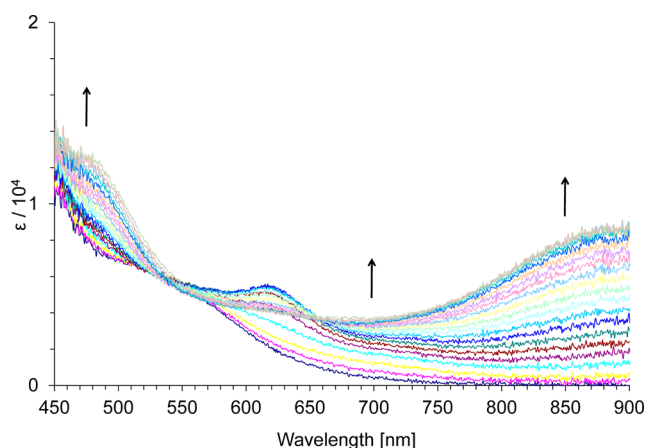


Figure 4. Continuous change in the UV-vis spectrum of **20** under constant-current electrochemical reduction (100 mA) in benzonitrile containing Et_4NClO_4 (0.1 M) at 30 s intervals.

reversibility of the color changes of **19** and **20** under the redox cycle was improved by introducing a 6-azulenyl group in the molecule. These results were attributed to the stabilization of anionic species generated by electrochemical reduction, because of the electron-withdrawing nature of the substituted 6-azulenyl group. The absorption band at around $\lambda_{\text{max}} = 520$ nm of **21** gradually decreased with the development of new absorption bands in the near-infrared region along with two isosbestic points during the electrochemical reduction. The reversible oxidation of the reduced species did not regenerate the spectrum of the starting material, although TCBDs with a 6-azulenyl group **19** and **20** showed reversible color changes. The poor reversibility of the color change of **21** was ascribed to the instability of the presumed dianionic species under the conditions of the spectroscopic measurements, because of the electron-donating property of the 2-amino group on the 6-azulenyl substituent. On the whole, TCBDs with two-azulenyl substituents **17–20** revealed a higher reversibility of color change under the electrochemical reduction conditions, compared to that of TCBD with phenyl substituent **27**. These results should be attributable to the stabilization of anionic species by 2-azulenyl and 6-azulenyl groups substituted to the TCBD unit.

The longest wavelength absorption bands of the DCNQ derivatives **22–26** gradually decreased during the electrochemical reduction. However, the reversible oxidation of the obtained yellow-colored solution did not regenerate the original spectra of the corresponding starting compounds. The longest wavelength absorption band of **22** gradually decreased, and the color of the solution changed from blue to yellow during the electrochemical reduction. Reverse oxidation of the reduced species of **22** did not completely regenerate the blue color and the spectra of the corresponding original compound. The greenish-blue color of the solution of **23** changed to yellow during electrochemical reduction along with a decrement of the absorption band at around $\lambda_{\text{max}} = 650$ nm, and the reverse oxidation of the yellow-colored solution regenerated the

original color of **23** (Figure 5). The longest wavelength absorption bands of **24** and **25** gradually decreased along with

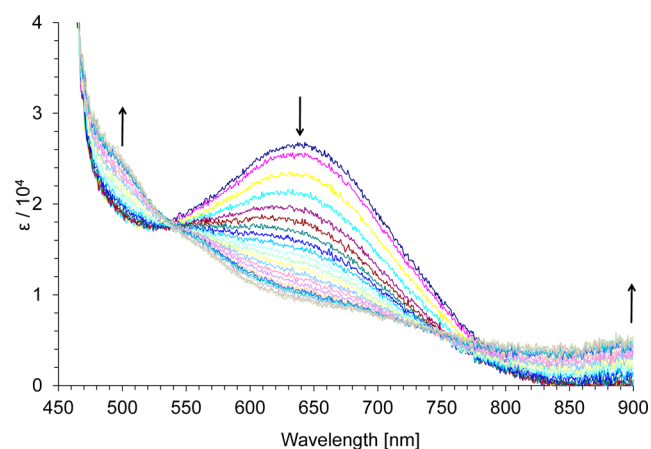


Figure 5. Continuous change in the UV-vis spectrum of **23** under the constant-current electrochemical reduction (100 mA) in benzonitrile containing Et_4NClO_4 (0.1 M) at 30 s intervals.

the development of new absorption bands in the near-infrared region with two isosbestic points during the electrochemical reduction. Reverse oxidation of the reduced solutions did not regenerate the original spectra of **24** and **25**. The color of the solution of **26** changed from green to yellow under the electrochemical reduction with the decrement of an original absorption band in the visible region. However, reverse oxidation of the yellow colored solution did not regenerate the original spectrum of **26**.

From the results described above, TCBD derivatives **17–21** substituted by a 2-azulenyl or 6-azulenyl group displayed a reversible color change under the electrochemical conditions, although the corresponding DCNQ derivatives exhibited poor reversibility in the color changes. It is well-known that the radical anion of DCNQ derivatives readily dimerizes or polymerizes to form a σ -bond between the two DCNQ moieties. Thus, the irreversibility of the color changes of the DCNQ derivatives may be caused by σ -bond formation between the intermediary radical anions formed in the electrochemical reduction.

CONCLUSIONS

Di(azulenyl)acetylenes **8–13** were prepared by palladium-catalyzed Sonogashira–Hagihara reactions. A series of TCBDs **17–21** and DCNQs **22–26** bearing two azulene substituents were synthesized by a formal [2 + 2] cycloaddition reaction of **8–13** with TCNE and TCNQ, respectively, followed by ring-opening reaction of the initially formed cyclobutene derivatives. Intramolecular CT absorption bands were found in the UV-vis spectra of the novel chromophores **17–26**. An analysis by CV and DPV showed that TCBDs **17–21** and DCNQs **22–26** exhibited a reversible two-stage reduction wave, due to the electrochemical reduction of TCBD and DCNQ moieties. Color changes were also observed during the electrochemical reduction. In particular, TCBDs **17–20** possessing a 2-azulenyl or 6-azulenyl substituent exhibited color changes with high reversibility, attributable to the stabilization of anionic species during the electrochemical reaction. In contrast to the results on the TCBD derivatives, most of the DCNQ derivatives showed poor reversibility in their electrochromic behavior,

although a significant color change was observed during the electrochemical reduction.

To evaluate the scope of this class of molecules, the preparation of novel donor–acceptor chromophores connected to various π -electron systems is now in progress in our laboratory.

EXPERIMENTAL SECTION

General Methods. ^1H and ^{13}C NMR spectra were measured at 500 MHz (^1H NMR) and 125 MHz (^{13}C NMR), respectively. Voltammetry measurements were carried out in benzonitrile as a measurement solvent, with Pt working and auxiliary electrodes and a reference electrode formed from Ag/AgNO₃ (0.01 M) in acetonitrile containing tetrabutylammonium perchlorate (0.1 M).

(2-Azulenyl)(5-isopropyl-3-methoxycarbonyl-1-azulenyl)acetylene (9). The reaction of 7 (252 mg, 1.00 mmol) with 2 (279 mg, 1.10 mmol) in triethylamine (10 mL) and THF (10 mL) in the presence of CuI (38 mg, 0.10 mmol) and tetrakis(triphenylphosphine)palladium(0) (58 mg, 0.05 mmol) at 50 °C for 1 h followed by column chromatography on silica gel with CH₂Cl₂ afforded 9 (375 mg, 99%) as dark blue crystals: mp 128.0–130.0 °C (AcOEt); IR (KBr disk) ν_{max} = 2183 (C≡C), 1687 (C=O) cm⁻¹; UV–vis (CH₂Cl₂) λ_{max} (log ϵ) = 239 (4.55), 283 sh (4.78), 293 (4.81), 313 sh (4.74), 435 (4.52), 457 (4.59), 573 (3.17), 617 sh (3.07), 680 sh (2.58) nm; ^1H NMR (500 MHz, CDCl₃) δ_{H} = 9.74 (d, 1H, J = 1.5 Hz, H₄), 8.76 (d, 1H, J = 10.0 Hz, H₈), 8.53 (s, 1H, H₂), 8.25 (d, 2H, J = 10.0 Hz, H_{4',8'}), 7.83 (d, 1H, J = 10.0 Hz, H₆), 7.57–7.50 (m, 4H, H_{7,1',3',6'}), 7.19 (t, 2H, J = 10.0 Hz, H_{5,7'}), 3.97 (s, 3H, CO₂Me), 3.24 (sept, 1H, J = 7.0 Hz, *i*Pr), 1.43 (d, 6H, J = 7.0 Hz, *i*Pr) ppm; ^{13}C NMR (125 MHz, CDCl₃) δ_{C} = 165.5 (CO₂Me), 150.8 (C₅), 145.0 (C_{3a}), 143.0 (C₂), 141.5 (C_{8a}), 140.4 (C_{3a',8a'}), 139.4 (C₆), 138.4 (C₄), 136.9 (C_{6'}), 136.4 (C₈), 135.9 (C_{4',8'}), 131.2 (C_{2'}), 127.7 (C_{7'}), 124.0 (C_{5',7'}), 120.3 (C_{1',3'}), 115.4 (C₃), 109.4 (C₁), 92.6 (C≡C), 91.7 (C≡C), 51.2 (CO₂Me), 39.3 (*i*Pr), 24.6 (*i*Pr) ppm; HRMS (ESI–TOF, positive) Calcd for C₂₇H₂₂O₂ + Na⁺ [M + Na]⁺ 401.1512, found 401.1512. Anal. Calcd for C₂₇H₂₂O₂·1/4H₂O: C, 84.68; H, 5.92. Found: C, 84.76; H, 5.92.

(1,3-Bisethoxycarbonyl-2-azulenyl)(5-isopropyl-3-methoxycarbonyl-1-azulenyl)acetylene (10). The reaction of 7 (252 mg, 1.00 mmol) with 3 (337 mg, 1.10 mmol) in triethylamine (10 mL) and THF (10 mL) in the presence of CuI (38 mg, 0.10 mmol) and tetrakis(triphenylphosphine)palladium(0) (58 mg, 0.05 mmol) at 50 °C for 6 h followed by column chromatography on silica gel with CH₂Cl₂ afforded 10 (481 mg, 92%) as red crystals: mp 122.0–123.0 °C (EtOH); IR (KBr disk) ν_{max} = 2177 (C≡C), 1689 (C=O) cm⁻¹; UV–vis (CH₂Cl₂) λ_{max} (log ϵ) = 240 (4.54), 275 sh (4.52), 298 sh (4.64), 321 (4.74), 355 sh (4.38), 408 sh (4.06), 477 (4.51) nm; ^1H NMR (500 MHz, CDCl₃) δ_{H} = 9.76 (s, 1H, H₄), 9.60 (d, 2H, J = 10.0 Hz, H_{4',8'}), 9.07 (d, 1H, J = 10.0 Hz, H₈), 8.53 (s, 1H, H₂), 7.86 (d, 1H, J = 10.0 Hz, H₆), 7.84 (t, 1H, J = 10.0 Hz, H_{6'}), 7.68 (t, 2H, J = 10.0 Hz, H_{5,7'}), 7.60 (t, 1H, J = 10.0 Hz, H₇), 4.58 (q, 4H, J = 6.0 Hz, CO₂Et), 3.98 (s, 3H, CO₂Me), 3.26 (sept, 1H, J = 7.0 Hz, *i*Pr), 1.49 (t, 6H, J = 6.0 Hz, CO₂Et), 1.45 (d, 6H, J = 7.0 Hz, *i*Pr) ppm; ^{13}C NMR (125 MHz, CDCl₃) δ_{C} = 165.4 (CO₂Me), 165.1 (CO₂Et), 151.2 (C₅), 146.0 (C_{3a}), 143.4 (C_{3a',8a'}), 142.9 (C₂), 141.8 (C_{8a}), 139.7 (C₆ or C_{6'}), 139.7 (C₆ or C_{6'}), 138.5 (C₄), 138.0 (C_{4',8'}), 137.3 (C₈), 134.7 (C_{2'}), 130.8 (C_{5',7'}), 128.2 (C₇), 118.6 (C_{1',3'}), 115.8 (C₃), 109.8 (C₁), 101.4 (C≡C), 92.5 (C≡C), 60.4 (CO₂Et), 51.3 (CO₂Me), 39.3 (*i*Pr), 24.6 (*i*Pr), 14.8 (CO₂Et) ppm; HRMS (ESI–TOF, positive) Calcd for C₃₃H₃₀O₆ + Na⁺ [M + Na]⁺ 545.1935, found 545.1935. Anal. Calcd for C₃₃H₃₀O₆: C, 75.84; H, 5.79. Found: C, 75.77; H, 5.89.

(6-Azulenyl)(5-isopropyl-3-methoxycarbonyl-1-azulenyl)acetylene (11). The reaction of 7 (252 mg, 1.00 mmol) with 4 (228 mg, 1.10 mmol) in triethylamine (10 mL) and THF (10 mL) in the presence of CuI (38 mg, 0.10 mmol) and tetrakis(triphenylphosphine)palladium(0) (58 mg, 0.05 mmol) at 50 °C for 6 h followed by column chromatography on silica gel with CH₂Cl₂ afforded 11 (375 mg, 99%) as dark blue crystals: mp 148.0–149.0 °C (AcOEt); IR (KBr disk) ν_{max} = 2222 (C≡C), 1686 (C=O) cm⁻¹;

UV–vis (CH₂Cl₂) λ_{max} (log ϵ) = 241 (4.67), 292 (4.92), 309 sh (4.79), 323 sh (4.69), 347 sh (4.33), 430 sh (4.66), 454 (4.72), 568 (3.15), 613 sh (3.08), 680 sh (2.67), 748 sh (2.04) nm; ^1H NMR (500 MHz, CDCl₃) δ_{H} = 9.75 (d, 1H, J = 1.5 Hz, H₄), 8.71 (d, 1H, J = 10.0 Hz, H₈), 8.51 (s, 1H, H₂), 8.26 (d, 2H, J = 10.0 Hz, H_{4',8'}), 7.85 (d, 1H, J = 10.0 Hz, H₆), 7.85 (t, 1H, J = 4.0 Hz, H_{2'}), 7.57 (dd, 1H, J = 10.0, 10.0 Hz, H₇), 7.49 (d, 2H, J = 10.0 Hz, H_{5,7'}), 7.38 (d, 2H, J = 4.0 Hz, H_{1',3'}), 3.97 (s, 3H, CO₂Me), 3.25 (sept, 1H, J = 7.0 Hz, *i*Pr), 1.45 (d, 6H, J = 7.0 Hz, *i*Pr) ppm; ^{13}C NMR (125 MHz, CDCl₃) δ_{C} = 165.3 (CO₂Me), 151.2 (C₅), 145.2 (C_{3a}), 143.1 (C₂), 141.7 (C_{8a}), 139.6 (C₆), 139.4 (C_{3a',8a'}), 138.6 (C₄), 136.9 (C_{2'}), 136.3 (C₈), 135.0 (C_{4',8'}), 133.2 (C_{6'}), 127.9 (C₇), 125.6 (C_{5',7'}), 118.9 (C_{1',3'}), 115.6 (C₃), 108.6 (C₁), 99.1 (C≡C), 88.3 (C≡C), 51.2 (CO₂Me), 39.3 (*i*Pr), 24.6 (*i*Pr) ppm. HRMS (ESI–TOF, positive) Calcd for C₂₇H₂₂O₂ + Na⁺ [M + Na]⁺ 401.1512, found 401.1512. Anal. Calcd for C₂₇H₂₂O₂: C, 85.69; H, 5.86. Found: C, 85.51; H, 5.99.

(1,3-Bisethoxycarbonyl-6-azulenyl)(5-isopropyl-3-methoxycarbonyl-1-azulenyl)acetylene (12). The reaction of 7 (252 mg, 1.00 mmol) with 5 (386 mg, 1.10 mmol) in triethylamine (10 mL) and THF (10 mL) in the presence of CuI (38 mg, 0.10 mmol) and tetrakis(triphenylphosphine)palladium(0) (58 mg, 0.05 mmol) at 50 °C for 1 h followed by column chromatography on silica gel with CH₂Cl₂ afforded 12 (517 mg, 99%) as reddish brown crystals: mp 193.0–194.0 °C (AcOEt); IR (KBr disk) ν_{max} = 2179 (C≡C), 1689 (C=O) cm⁻¹; UV–vis (CH₂Cl₂) λ_{max} (log ϵ) = 240 (4.83), 272 (4.60), 310 (4.67), 328 (4.72), 352 sh (4.46), 377 (4.39), 477 (4.72) nm; ^1H NMR (500 MHz, CDCl₃) δ_{H} = 9.78 (d, 1H, J = 1.5 Hz, H₄), 9.64 (d, 2H, J = 11.0 Hz, H_{4',8'}), 8.72 (s, 1H, H₂), 8.71 (d, 1H, J = 10.0 Hz, H₈), 8.54 (s, 1H, H₂), 7.94 (d, 2H, J = 11.0 Hz, H_{5,7'}), 7.90 (d, 1H, J = 10.0 Hz, H₆), 7.64 (dd, 1H, J = 10.0, 10.0 Hz, H₇), 4.43 (q, 4H, J = 7.0 Hz, CO₂Et), 3.98 (s, 3H, CO₂Me), 3.28 (sept, 1H, J = 7.0 Hz, *i*Pr), 1.46 (d, 6H, J = 7.0 Hz, *i*Pr), 1.45 (t, 6H, J = 7.0 Hz, CO₂Et) ppm; ^{13}C NMR (125 MHz, CDCl₃) δ_{C} = 165.2 (CO₂Me), 165.0 (CO₂Et), 151.9 (C₅), 145.6 (C_{3a}), 143.6 (C₂), 142.9 (C_{2'}), 142.8 (C_{3a',8a'}), 142.1 (C_{8a}), 139.9 (C₆), 138.8 (C₄), 137.6 (C_{6'}), 137.5 (C_{4',8'}), 136.3 (C₈), 132.7 (C_{5',7'}), 128.5 (C₇), 116.8 (C_{1',3'}), 116.0 (C₃), 107.7 (C₁), 98.6 (C≡C), 92.8 (C≡C), 60.1 (CO₂Et), 51.3 (CO₂Me), 39.3 (*i*Pr), 24.6 (*i*Pr), 14.6 (CO₂Et) ppm. HRMS (ESI–TOF, positive) Calcd for C₃₃H₃₀O₆ + Na⁺ [M + Na]⁺ 545.1935, found 545.1935. Anal. Calcd for C₃₃H₃₀O₆: C, 75.84; H, 5.79. Found: C, 75.74; H, 5.78.

(2-Amino-1,3-bisethoxycarbonyl-6-azulenyl)(5-isopropyl-3-methoxycarbonyl-1-azulenyl)acetylene (13). The reaction of 7 (252 mg, 1.00 mmol) with 6 (403 mg, 1.10 mmol) in triethylamine (10 mL) and THF (10 mL) in the presence of CuI (38 mg, 0.10 mmol) and tetrakis(triphenylphosphine)palladium(0) (58 mg, 0.05 mmol) at 50 °C for 3 h followed by column chromatography on silica gel with CH₂Cl₂ afforded 13 (495 mg, 92%) as reddish brown crystals: mp 213.0–214.0 °C (AcOEt); IR (KBr disk) ν_{max} = 2219 (C≡C), 1691 (C=O) cm⁻¹; UV–vis (CH₂Cl₂) λ_{max} (log ϵ) = 249 (4.80), 286 (4.54), 315 (4.62), 337 (4.80), 375 sh (4.40), 396 (4.47), 460 sh (4.68), 482 (4.74), 580 sh (3.12), 627 sh (2.89) nm; ^1H NMR (500 MHz, CDCl₃) δ_{H} = 9.74 (d, 1H, J = 1.5 Hz, H₄), 9.03 (d, 2H, J = 11.0 Hz, H_{4',8'}), 8.67 (d, 1H, J = 10.0 Hz, H₈), 8.48 (s, 1H, H₂), 7.83 (d, 1H, J = 10.0 Hz, H₆), 7.83 (br s, 2H, NH₂), 7.80 (d, 2H, J = 11.0 Hz, H_{5,7'}), 7.55 (dd, 1H, J = 10.0, 10.0 Hz, H₇), 4.47 (q, 4H, J = 7.0 Hz, CO₂Et), 3.97 (s, 3H, CO₂Me), 3.25 (sept, 1H, J = 7.0 Hz, *i*Pr), 1.49 (d, 6H, J = 7.0 Hz, *i*Pr), 1.44 (t, 6H, J = 7.0 Hz, CO₂Et) ppm; ^{13}C NMR (125 MHz, CDCl₃) δ_{C} = 166.4 (CO₂Et), 165.3 (CO₂Me), 162.3 (C_{6'}), 151.2 (C₅), 145.2 (C_{3a',8a'}), 145.1 (C_{3a}), 143.0 (C₂), 141.6 (C_{8a}), 139.6 (C₆), 138.5 (C₄), 136.2 (C₈), 135.0 (C_{5',7'}), 130.0 (C_{4',8'}), 128.8 (C_{2'}), 127.8 (C₇), 115.5 (C₃), 108.6 (C₁), 100.5 (C_{1',3'}), 98.0 (C≡C), 88.2 (C≡C), 59.9 (CO₂Et), 51.3 (CO₂Me), 39.3 (*i*Pr), 24.6 (*i*Pr), 14.7 (CO₂Et) ppm. HRMS (FAB–TOF, positive) Calcd for C₃₃H₃₁NO₆⁺ [M]⁺ 537.2146, found 537.2142. Anal. Calcd for C₃₃H₃₁NO₆·1/2H₂O: C, 72.51; H, 5.90; N, 2.56. Found: C, 72.52; H, 5.92; N 2.52.

1,1,4,4-Tetracyano-2-(5-isopropyl-3-methoxycarbonyl-1-azulenyl)butadiene (14). TCNE (77 mg, 0.60 mmol) was added to a solution of 7 (126 mg, 0.50 mmol) in ethyl acetate (5 mL). The

resulting mixture was stirred at room temperature for 2 h under an Ar atmosphere. The solvent was removed under reduced pressure. The residue was purified by column chromatography on silica gel with CH_2Cl_2 /ethyl acetate (20:1) as an eluent to give **14** (179 mg, 94%) as purple crystals: mp 164.0–165.0 °C (CH_2Cl_2 /hexane); IR (KBr disk) $\nu_{\text{max}} = 2230$ ($\text{C}\equiv\text{N}$), 1695 ($\text{C}=\text{O}$) cm^{-1} ; UV–vis (CH_2Cl_2) λ_{max} (log ϵ) = 236 (4.38), 286 sh (4.54), 299 (4.56), 361 (4.03), 560 (3.83) nm; ^1H NMR (500 MHz, CDCl_3) $\delta_{\text{H}} = 10.02$ (s, 1H, H_4), 8.38 (s, 1H, H_2), 8.29 (s, 1H, TCBD), 8.20 (d, 1H, $J = 10.0$ Hz, H_8), 8.11 (d, 1H, $J = 10.0$ Hz, H_6), 7.86 (dd, 1H, $J = 10.0, 10.0$ Hz, H_7), 3.98 (s, 3H, CO_2Me), 3.34 (sept, 1H, $J = 7.0$ Hz, $i\text{Pr}$), 1.47 (d, 6H, $J = 7.0$ Hz, $i\text{Pr}$) ppm; ^{13}C NMR (125 MHz, CDCl_3) $\delta_{\text{C}} = 164.5$ (CO_2Me), 156.1 (C_8), 155.3 ($\text{C}=\text{C}(\text{CN})_2$), 155.2 (C_3), 145.4 (C_{8a}), 142.4 (C_2), 142.2 (C_4), 142.0 (C_{3a}), 141.0 (C_6), 136.0 ($\text{C}=\text{C}(\text{CN})_2$), 131.5 (C_7), 119.1 (C_3), 117.3 (C_1), 113.0 (CN), 112.2 (CN), 111.7 (CN), 108.6 (CN), 98.1 ($\text{C}(\text{CN})_2$), 85.4 ($\text{C}(\text{CN})_2$), 51.7 (CO_2Me), 39.5 ($i\text{Pr}$), 24.5 ($i\text{Pr}$) ppm; HRMS (FAB–TOF, positive) Calcd for $\text{C}_{23}\text{H}_{16}\text{N}_4\text{O}_2$ $[\text{M}]^+$ 380.1268, found 380.1280. Anal. Calcd for $\text{C}_{23}\text{H}_{16}\text{N}_4\text{O}_2 \cdot 1/10\text{H}_2\text{O}$: C, 72.28; H, 4.27; N, 14.66. Found: C, 72.25; H, 4.36; N, 14.60.

Compound (15). TCNQ (153 mg, 0.75 mmol) was added to a solution of **7** (126 mg, 0.50 mmol) in ethyl acetate (5 mL). The resulting mixture was heated at refluxing temperature for 6 h under an Ar atmosphere. The solvent was removed under reduced pressure. The residue was purified by column chromatography on silica gel with CH_2Cl_2 /ethyl acetate (15:1) as an eluent to give **15** (194 mg, 85%) as deep blue crystals: mp 147.0–148.0 °C (CH_2Cl_2 /hexane); IR (KBr disk) $\nu_{\text{max}} = 2226$ ($\text{C}\equiv\text{N}$), 1698 ($\text{C}=\text{O}$) cm^{-1} ; UV–vis (CH_2Cl_2) λ_{max} (log ϵ) = 239 (4.34), 297 (4.40), 395 sh (4.29), 416 (4.33), 443 (4.30), 510 (4.00), 709 (4.07) nm; ^1H NMR (500 MHz, CDCl_3) $\delta_{\text{H}} = 9.96$ (s, 1H, H_4), 8.38 (s, 1H, H_2), 8.27 (s, 1H, DCNQ), 7.97 (d, 1H, $J = 10.0$ Hz, H_6), 7.98 (d, 1H, $J = 10.0$ Hz, H_8), 7.60 (dd, 1H, $J = 9.5, 1.5$ Hz, DCNQ), 7.57 (dd, 1H, $J = 10.0, 10.0$ Hz, H_7), 7.45 (dd, 1H, $J = 9.5, 1.5$ Hz, DCNQ), 7.20 (dd, 1H, $J = 9.5, 1.5$ Hz, DCNQ), 6.90 (dd, 1H, $J = 9.5, 1.5$ Hz, DCNQ), 3.98 (s, 3H, CO_2Me), 3.31 (sept, 1H, $J = 7.0$ Hz, $i\text{Pr}$), 1.47 (d, 6H, $J = 7.0$ Hz, $i\text{Pr}$) ppm; ^{13}C NMR (125 MHz, CDCl_3) $\delta_{\text{C}} = 164.9$ (CO_2Me), 154.9 (C_2), 153.8 (C_3), 152.5 ($\text{C}=\text{C}(\text{CN})_2$), 143.79 ($\text{C}=\text{C}(\text{CN})_2$), 143.76 (C_{3a} or DCNQ), 143.7 (C_{3a} or DCNQ), 141.0 (C_6), 140.3 (C_4), 138.1 (C_{8a}), 135.7 (DCNQ), 135.2 (C_8), 131.1 (DCNQ), 129.9 (C_7), 127.6 (DCNQ), 127.0 (DCNQ), 121.3 (DCNQ), 118.0 (C_3), 113.9 (CN), 113.5 (CN), 113.4 (CN), 110.1 (C_1), 92.1 ($\text{C}(\text{CN})_2$), 79.7 ($\text{C}(\text{CN})_2$), 51.6 (CO_2Me), 39.4 ($i\text{Pr}$), 24.6 ($i\text{Pr}$) ppm; The signal of CN is overlapped with the other signals. HRMS (FAB–TOF, positive) Calcd for $\text{C}_{29}\text{H}_{20}\text{N}_4\text{O}_2$ $[\text{M}]^+$ 456.1581, found 456.1589. Anal. Calcd for $\text{C}_{29}\text{H}_{20}\text{N}_4\text{O}_2$: C, 76.30; H, 4.42; N, 12.27. Found: C, 76.19; H, 4.58; N, 12.21.

2-(2-Azulenyl)-1,1,4,4-tetracyano-3-(5-isopropyl-3-methoxycarbonyl-1-azulenyl)butadiene (17). TCNE (77 mg, 0.60 mmol) was added to a solution of **9** (189 mg, 0.50 mmol) in ethyl acetate (5 mL). The resulting mixture was stirred at room temperature for 2 h under an Ar atmosphere. The solvent was removed under reduced pressure. The residue was purified by column chromatography on silica gel with CH_2Cl_2 /ethyl acetate (20:1) with an eluent to give **17** (236 mg, 93%) as reddish brown crystals: mp 149.0–154.0 °C (AcOEt); IR (KBr disk) $\nu_{\text{max}} = 2221$ ($\text{C}\equiv\text{N}$), 1701 ($\text{C}=\text{O}$) cm^{-1} ; UV–vis (CH_2Cl_2) λ_{max} (log ϵ) = 257 (4.64), 309 (4.68), 410 (4.56), 420 sh (4.55), 509 sh (3.95), 556 sh (3.66), 703 sh (2.98), 763 (2.85) nm; UV–vis (10% CH_2Cl_2 /hexane) λ_{max} (log ϵ) = 253 (4.64), 308 (4.71), 401 (4.49), 420 sh (4.55), 510 sh (3.81), 548 sh (3.53), 690 sh (2.89), 771 (2.70) nm; ^1H NMR (500 MHz, CDCl_3) $\delta_{\text{H}} = 9.99$ (s, 1H, H_4), 8.54 (d, 1H, $J = 10.0$ Hz, H_8), 8.47 (d, 2H, $J = 10.0$ Hz, $\text{H}_{4,8}$), 8.25 (s, 1H, H_2), 8.13 (d, 1H, $J = 10.0$ Hz, H_6), 7.95 (t, 1H, $J = 10.0$ Hz, H_6), 7.93 (s, 2H, $\text{H}_{1,3}$), 7.79 (dd, 1H, $J = 10.0, 10.0$ Hz, H_7), 7.30 (t, 2H, $J = 10.0$ Hz, $\text{H}_{5,7}$), 3.89 (s, 3H, CO_2Me), 3.35 (sept, 1H, $J = 7.0$ Hz, $i\text{Pr}$), 1.48 (d, 6H, $J = 7.0$ Hz, $i\text{Pr}$) ppm; ^{13}C NMR (125 MHz, CDCl_3) $\delta_{\text{C}} = 164.5$ (CO_2Me), 163.7 ($\text{C}=\text{C}(\text{CN})_2$), 161.6 ($\text{C}=\text{C}(\text{CN})_2$), 156.5 (C_5), 146.0 (C_{8a}), 143.3 (C_7), 143.1 ($\text{C}_{4,8}$), 142.7 (C_2), 142.1 (C_6), 142.0 (C_{3a}), 141.1 (C_4), 140.6 ($\text{C}_{3a,8a}$), 137.7 (C_8), 137.6 (C_2), 131.9 (C_6), 126.1 ($\text{C}_{5,7}$), 119.6 ($\text{C}_{1,3}$), 119.5 (C_3), 119.3 (C_1), 113.9 (CN), 113.2 (CN), 112.5 (CN), 112.1 (CN), 84.5

($\text{C}(\text{CN})_2$), 80.8 ($\text{C}(\text{CN})_2$), 51.5 (CO_2Me), 39.5 ($i\text{Pr}$), 24.5 ($i\text{Pr}$) ppm; HRMS (ESI–TOF, positive) Calcd for $\text{C}_{33}\text{H}_{22}\text{N}_4\text{O}_2 + \text{Na}^+ [\text{M} + \text{Na}]^+$ 529.1635, found 529.1635. Anal. Calcd for $\text{C}_{33}\text{H}_{22}\text{N}_4\text{O}_2 \cdot 2/3\text{H}_2\text{O}$: C, 76.43; H, 4.54; N, 10.80. Found: C, 76.40; H, 4.62; N, 10.75.

2-(1,3-Bisethoxycarbonyl-2-azulenyl)-1,1,4,4-tetracyano-3-(5-isopropyl-3-methoxycarbonyl-1-azulenyl)butadiene (18). The procedure used for the preparation of **17** was adopted here. The reaction of **10** (261 mg, 0.50 mmol) with TCNE (77 mg, 0.60 mmol) in ethyl acetate (5 mL) at room temperature for 6 h afforded **18** (290 mg, 89%) as purple crystals: mp 101.0–103.0 °C (AcOEt/hexane); IR (KBr disk) $\nu_{\text{max}} = 2219$ ($\text{C}\equiv\text{N}$), 1691 ($\text{C}=\text{O}$) cm^{-1} ; UV–vis (CH_2Cl_2) λ_{max} (log ϵ) = 236 (4.73), 306 (4.88), 363 (4.39), 392 sh (4.09), 558 (3.84) nm; UV–vis (10% CH_2Cl_2 /hexane) λ_{max} (log ϵ) = 235 (4.75), 306 (4.89), 363 (4.39), 390 sh (4.11), 557 (3.85) nm; ^1H NMR (500 MHz, CDCl_3) $\delta_{\text{H}} = 10.02$ (d, 1H, $J = 1.5$ Hz, H_4), 9.87 (d, 2H, $J = 10.0$ Hz, $\text{H}_{4,8}$), 8.91 (s, 1H, H_2), 8.40 (d, 1H, $J = 10.0$ Hz, H_8), 8.18 (t, 1H, $J = 10.0$ Hz, H_6), 8.06 (d, 1H, $J = 10.0$ Hz, H_6), 7.92 (t, 2H, $J = 10.0$ Hz, $\text{H}_{5,7}$), 7.86 (dd, 1H, $J = 10.0, 10.0$ Hz, H_7), 4.55 (q, 4H, $J = 7.0$ Hz, CO_2Et), 4.01 (s, 3H, CO_2Me), 3.33 (sept, 1H, $J = 7.0$ Hz, $i\text{Pr}$), 1.50–1.47 (m, 12H, CO_2Et , $i\text{Pr}$) ppm; ^{13}C NMR (125 MHz, CDCl_3) $\delta_{\text{C}} = 167.2$ ($\text{C}=\text{C}(\text{CN})_2$), 165.1 (CO_2Me), 163.9 (CO_2Et), 158.4 ($\text{C}=\text{C}(\text{CN})_2$), 154.6 (C_5), 144.9 (C_2), 144.8 (C_2), 144.7 (C_{8a}), 143.9 (C_6), 142.7 ($\text{C}_{4,8}$), 142.4 ($\text{C}_{3a,8a}$), 142.2 (C_{3a}), 141.2 (C_6), 140.4 (C_4), 135.9 (C_8), 132.1 ($\text{C}_{5,7}$), 131.1 (C_7), 121.1 (C_1), 118.5 (C_3), 114.6 (CN), 112.7 (CN), 111.1 (CN), 110.0 (CN), 95.4 ($\text{C}(\text{CN})_2$), 85.3 ($\text{C}(\text{CN})_2$), 61.6 (CO_2Et), 51.5 (CO_2Me), 39.4 ($i\text{Pr}$), 24.5 ($i\text{Pr}$), 14.5 (CO_2Et) ppm; The signals of $\text{C}_{1'}$ and $\text{C}_{3'}$ are overlapped with the other signals. HRMS (FAB–TOF, positive) Calcd for $\text{C}_{39}\text{H}_{30}\text{N}_4\text{O}_6$ $[\text{M}]^+$ 650.2160, found 650.2160. Anal. Calcd for $\text{C}_{39}\text{H}_{30}\text{N}_4\text{O}_6$: C, 71.99; H, 4.65; N, 8.61. Found: C, 71.81; H, 4.75; N, 8.53.

2-(6-Azulenyl)-1,1,4,4-tetracyano-3-(5-isopropyl-3-methoxycarbonyl-1-azulenyl)butadiene (19). The procedure used for the preparation of **17** was adopted here. The reaction of **11** (189 mg, 0.50 mmol) with TCNE (77 mg, 0.60 mmol) in ethyl acetate (5 mL) at room temperature for 3 h afforded **19** (233 mg, 92%) as reddish brown crystals: mp 146.0–149.0 °C (AcOEt/hexane); IR (KBr disk) $\nu_{\text{max}} = 2221$ ($\text{C}\equiv\text{N}$), 1700 ($\text{C}=\text{O}$) cm^{-1} ; UV–vis (CH_2Cl_2) λ_{max} (log ϵ) = 268 (4.61), 299 (4.81), 412 (4.28), 545 sh (3.88) nm; UV–vis (10% CH_2Cl_2 /hexane) λ_{max} (log ϵ) = 242 (4.54), 265 (4.59), 297 (4.82), 409 (4.27), 452 sh (4.02), 513 sh (3.85), 552 sh (3.71) nm; ^1H NMR (500 MHz, CDCl_3) $\delta_{\text{H}} = 10.01$ (d, 1H, $J = 1.5$ Hz, H_4), 8.46 (d, 1H, $J = 10.0$ Hz, H_8), 8.41 (d, 2H, $J = 10.0$ Hz, $\text{H}_{4,8}$), 8.36 (s, 1H, H_2), 8.15 (d, 1H, $J = 10.0$ Hz, H_6), 8.14 (t, 1H, $J = 4.0$ Hz, H_2), 7.98 (dd, 1H, $J = 10.0, 10.0$ Hz, H_7), 7.55 (d, 2H, $J = 4.0$ Hz, $\text{H}_{1,3}$), 7.39 (d, 2H, $J = 10.0$ Hz, $\text{H}_{5,7}$), 3.97 (s, 3H, CO_2Me), 3.35 (sept, 1H, $J = 7.0$ Hz, $i\text{Pr}$), 1.47 (d, 6H, $J = 7.0$ Hz, $i\text{Pr}$) ppm; ^{13}C NMR (125 MHz, CDCl_3) $\delta_{\text{C}} = 173.0$ (C_6), 164.3 (CO_2Me), 160.4 ($\text{C}=\text{C}(\text{CN})_2$), 157.0 (C_5), 146.1 (C_{8a}), 142.6 (C_6 or C_2), 142.6 (C_6 or C_2), 142.3 (C_2), 142.0 (C_{3a}), 140.9 ($\text{C}_{3a,8a}$), 140.9 (C_4), 139.3 ($\text{C}=\text{C}(\text{CN})_2$), 137.4 (C_8), 135.1 ($\text{C}_{4,8}$), 132.2 (C_7), 122.7 ($\text{C}_{5,7}$), 121.4 ($\text{C}_{1,3}$), 119.5 (C_3), 119.3 (C_1), 113.6 (CN), 112.6 (CN), 111.6 (CN), 111.0 (CN), 91.1 ($\text{C}(\text{CN})_2$), 81.4 ($\text{C}(\text{CN})_2$), 51.7 (CO_2Me), 39.5 ($i\text{Pr}$), 24.5 ($i\text{Pr}$) ppm; HRMS (ESI–TOF, positive) Calcd for $\text{C}_{33}\text{H}_{22}\text{N}_4\text{O}_2 + \text{Na}^+ [\text{M} + \text{Na}]^+$ 529.1635, found 529.1635. Anal. Calcd for $\text{C}_{33}\text{H}_{22}\text{N}_4\text{O}_2$: C, 78.25; H, 4.38; N, 11.06. Found: C, 78.11; H, 4.47; N, 11.00.

2-(1,3-Bisethoxycarbonyl-6-azulenyl)-1,1,4,4-tetracyano-3-(5-isopropyl-3-methoxycarbonyl-1-azulenyl)butadiene (20). The procedure used for the preparation of **17** was adopted here. The reaction of **12** (261 mg, 0.50 mmol) with TCNE (77 mg, 0.60 mmol) in ethyl acetate (5 mL) at room temperature for 6 h afforded **20** (290 mg, 89%) as purple crystals: mp 101.0–103.0 °C (AcOEt/hexane); IR (KBr disk) $\nu_{\text{max}} = 2219$ ($\text{C}\equiv\text{N}$), 1691 ($\text{C}=\text{O}$) cm^{-1} ; UV–vis (CH_2Cl_2) λ_{max} (log ϵ) = 236 (4.73), 306 (4.88), 363 (4.39), 392 sh (4.09), 558 (3.84) nm; UV–vis (10% CH_2Cl_2 /hexane) λ_{max} (log ϵ) = 235 (4.75), 306 (4.89), 363 (4.39), 390 sh (4.11), 557 (3.85) nm; ^1H NMR (500 MHz, CDCl_3) $\delta_{\text{H}} = 10.04$ (d, 1H, $J = 1.5$ Hz, H_4), 9.81 (d, 2H, $J = 11.0$ Hz, $\text{H}_{4,8}$), 8.97 (s, 1H, H_2), 8.42 (d, 1H, $J = 10.0$ Hz, H_8), 8.36 (s, 1H, H_2), 8.18 (d, 1H, $J = 10.0$ Hz, H_6), 8.00 (t, 2H, J

= 11.0 Hz, H_{5,7}), 7.83 (dd, 1H, *J* = 10.0, 10.0 Hz, H₇), 4.44 (q, 4H, *J* = 7.0 Hz, CO₂Et), 3.98 (s, 3H, CO₂Me), 3.36 (sept, 1H, *J* = 7.0 Hz, *i*Pr), 1.47 (d, 6H, *J* = 7.0 Hz, *i*Pr), 1.44 (t, 6H, *J* = 7.0 Hz, CO₂Et) ppm; ¹³C NMR (125 MHz, CDCl₃) δ_C = 171.0 (C₆'), 164.2 (CO₂Me), 164.1 (CO₂Et), 159.3 (C=C(CN)₂), 157.4 (C₅'), 147.3 (C₂'), 146.3 (C_{8a}'), 143.9 (C_{3a',8a'}), 142.8 (C₆'), 142.2 (C_{3a}'), 142.0 (C=C(CN)₂), 142.0 (C₂'), 141.1 (C₄'), 137.9 (C_{4',8'}), 137.4 (C₈'), 132.4 (C₇'), 129.3 (C_{5',7'}), 119.8 (C₃'), 118.9 (C_{1',3'}'), 118.7 (C₁'), 113.3 (CN), 112.6 (CN), 111.0 (CN), 110.5 (CN), 93.1 (C(CN)₂), 81.3 (C(CN)₂), 60.7 (CO₂Et), 51.8 (CO₂Me), 39.5 (*i*Pr), 24.5 (*i*Pr), 14.5 (CO₂Et) ppm; HRMS (FAB–TOF, positive) Calcd for C₃₉H₃₀N₄O₆⁺ [M]⁺ 650.2160, found 650.2165. Anal. Calcd for C₃₉H₃₀N₄O₆: C, 71.99; H, 4.65; N, 8.61. Found: C, 71.81; H, 4.75; N, 8.53.

2-(2-Amino-1,3-bisethoxycarbonyl-6-azulenyl)-1,1,4,4-tetra-cyano-3-(5-isopropyl-3-methoxycarbonyl-1-azulenyl)-butadiene (21). The procedure used for the preparation of 17 was adopted here. The reaction of 13 (269 mg, 0.50 mmol) with TCNE (77 mg, 0.60 mmol) in ethyl acetate (5 mL) at room temperature for 3 h afforded 21 (299 mg, 90%) as purple crystals: mp 182.0–185.0 °C (AcOEt/hexane); IR (KBr disk) ν_{max} = 2222 (C≡N), 1686 (C=O) cm⁻¹; UV–vis (CH₂Cl₂) λ_{max} (log ε) = 246 (4.73), 309 (4.63), 343 (4.71), 414 (4.36), 522 (4.45) nm; UV–vis (10% CH₂Cl₂/hexane) λ_{max} (log ε) = 243 (4.74), 307 (4.61), 341 (4.72), 409 (4.35), 510 (4.44) nm; ¹H NMR (500 MHz, CDCl₃) δ_H = 10.03 (d, 1H, *J* = 1.5 Hz, H₄'), 9.06 (d, 2H, *J* = 11.5 Hz, H_{4',8'}'), 8.47 (d, 1H, *J* = 10.0 Hz, H₈'), 8.37 (s, 1H, H₂'), 8.34 (s, 2H, NH₂'), 8.17 (dd, 1H, *J* = 10.0, 1.5 Hz, H₆'), 7.99 (dd, 1H, *J* = 10.0, 10.0 Hz, H₇'), 7.77 (d, 2H, *J* = 11.5 Hz, H_{5',7'}'), 4.50 (q, 4H, *J* = 7.0 Hz, CO₂Et), 3.97 (s, 3H, CO₂Me), 3.36 (sept, 1H, *J* = 7.0 Hz, *i*Pr), 1.50 (d, 6H, *J* = 7.0 Hz, *i*Pr), 1.49 (t, 6H, *J* = 7.0 Hz, CO₂Et) ppm; ¹³C NMR (125 MHz, CDCl₃) δ_C = 171.8 (C₆'), 165.9 (CO₂Et), 165.3 (C=C(CN)₂), 164.4 (CO₂Me), 161.0 (C=C(CN)₂), 157.3 (C₅'), 147.0 (C_{3a',8a'}'), 146.3 (C_{8a}'), 142.7 (C₆'), 142.6 (C₂'), 142.1 (C_{3a}'), 140.9 (C₄'), 137.6 (C₈'), 134.1 (C₂'), 132.7 (C_{5',7'}'), 132.4 (C₇'), 128.4 (C_{4',8'}'), 120.2 (C₃'), 119.7 (C₁'), 113.8 (CN), 112.6 (CN), 112.3 (CN), 111.4 (CN), 102.9 (C_{1',3'}'), 88.2 (C(CN)₂), 80.9 (C(CN)₂), 60.7 (CO₂Et), 51.8 (CO₂Me), 39.6 (*i*Pr), 24.5 (*i*Pr), 14.6 (CO₂Et) ppm; HRMS (ESI–TOF, positive) Calcd for C₃₉H₃₁N₅O₆ + Na⁺ [M + Na]⁺ 688.2167, found 688.2166. Anal. Calcd for C₃₉H₃₁N₅O₆: C, 70.37; H, 4.69; N, 10.52. Found: C, 70.11; H, 4.83; N, 10.44.

Compound (22). TCNQ (102 mg, 0.50 mmol) was added to a solution of 8 (120 mg, 0.25 mmol) in ethyl acetate (5 mL). The resulting mixture was heated at refluxing temperature for 12 h under an Ar atmosphere. The solvent was removed under reduced pressure. The residue was purified by column chromatography on silica gel with CH₂Cl₂/ethyl acetate (10:1) as an eluent to give 22 (162 mg, 95%) as dark blue crystals: mp 198.0–201.0 °C (AcOEt); IR (KBr disk) ν_{max} = 2208 (C≡N), 1701 (C=O) cm⁻¹; UV–vis (CH₂Cl₂) λ_{max} (log ε) = 242 (4.72), 297 (4.71), 410 (4.53), 655 (4.48) nm; UV–vis (10% CH₂Cl₂/hexane) λ_{max} (log ε) = 241 (4.72), 296 (4.70), 404 (4.52), 611 (4.45) nm; ¹H NMR (500 MHz, CDCl₃) δ_H = 9.95 (d, 1H, *J* = 1.5 Hz, H₄'), 9.90 (d, 1H, *J* = 1.5 Hz, H₄'), 8.60 (s, 1H, H₂'), 8.54 (d, 1H, *J* = 10.0 Hz, H₈'), 8.36 (d, 1H, *J* = 10.0 Hz, H₈'), 8.33 (s, 1H, H₂'), 8.04 (d, 1H, *J* = 10.0 Hz, H₆'), 7.98 (d, 1H, *J* = 10.0 Hz, H₆'), 7.76 (dd, 1H, *J* = 10.0, 10.0 Hz, H₇'), 7.64 (dd, 1H, *J* = 10.0, 10.0 Hz, H₇'), 7.17 (br s, 2H, DCNQ), 7.00 (br s, 2H, DCNQ), 3.94 (s, 3H, CO₂Me), 3.93 (s, 3H, CO₂Me), 3.35–3.28 (m, 2H, *i*Pr), 1.46 (d, 6H, *J* = 7.0 Hz, *i*Pr), 1.44 (d, 6H, *J* = 7.0 Hz, *i*Pr) ppm; ¹³C NMR (125 MHz, CDCl₃) δ_C = 166.3 (C=C(CN)₂), 164.7 (CO₂Me), 164.6 (CO₂Me), 155.9 (C₅ or C_{5'}), 155.0 (C₅ or C_{5'}), 153.7 (C=C(CN)₂), 147.8 (DCNQ), 145.7 (C_{8a}'), 145.1 (DCNQ), 144.4 (C₂'), 144.0 (C_{8a}'), 143.3 (C₂'), 141.8 (C_{3a,6'}'), 141.7 (C_{3a'}'), 141.6 (C₆'), 140.4 (C₄'), 140.2 (C₄'), 136.5 (C₈'), 136.3 (C₈'), 134.7 (DCNQ), 133.9 (DCNQ), 131.4 (C₇'), 131.1 (C₇'), 126.0 (C₁'), 125.7 (DCNQ), 124.8 (DCNQ), 123.1 (C₁'), 119.1 (C₃'), 118.8 (C₃'), 115.0 (CN), 114.3 (CN), 114.2 (CN), 113.4 (CN), 82.3 (C(CN)₂), 73.9 (C(CN)₂), 51.7 (CO₂Me), 51.6 (CO₂Me), 39.4 (*i*Pr), 24.5 (*i*Pr) ppm; HRMS (ESI–TOF, positive) Calcd for C₄₄H₃₄N₄O₄ + Na⁺ [M + Na]⁺ 705.2473, found 705.2472. Anal. Calcd for C₄₄H₃₄N₄O₄·H₂O: C, 75.41; H, 5.18; N, 7.99. Found: C, 75.63; H, 5.20; N, 8.01.

Compound (23). The procedure used for the preparation of 22 was adopted here. The reaction of 9 (95 mg, 0.25 mmol) with TCNQ (102 mg, 0.50 mmol) in ethyl acetate (5 mL) at refluxing temperature for 16 h afforded 23 (136 mg, 93%) as dark blue crystals: mp 208.0–211.0 °C (AcOEt/hexane); IR (KBr disk) ν_{max} = 2207 (C≡N), 1700 (C=O) cm⁻¹; UV–vis (CH₂Cl₂) λ_{max} (log ε) = 315 (4.75), 385 sh (4.48), 405 (4.49), 433 sh (4.35), 631 (4.42) nm; UV–vis (10% CH₂Cl₂/hexane) λ_{max} (log ε) = 311 (4.78), 385 sh (4.48), 401 (4.50), 425 sh (4.36), 592 (4.39) nm; ¹H NMR (500 MHz, CDCl₃) δ_H = 9.90 (d, 1H, *J* = 2.0 Hz, H₄'), 8.43 (d, 1H, *J* = 10.0 Hz, H₈'), 8.38 (d, 2H, *J* = 10.0 Hz, H_{4',8'}'), 8.17 (s, 1H, H₂'), 8.00 (dd, 1H, *J* = 10.0, 2.0 Hz, H₆'), 7.78 (s, 1H, H_{1',3'}'), 7.73 (t, 1H, *J* = 10.0 Hz, H₆'), 7.67 (t, 1H, *J* = 10.0 Hz, H₇'), 7.30–7.20 (m, 4H, H_{5',7'} and DCNQ), 7.09 (dd, 1H, *J* = 9.5, 1.5 Hz, DCNQ), 7.01 (dd, 1H, *J* = 9.5, 1.5 Hz, DCNQ), 3.90 (s, 3H, CO₂Me), 3.31 (sept, 1H, *J* = 7.0 Hz, *i*Pr), 1.47 (d, 6H, *J* = 7.0 Hz, *i*Pr) ppm; ¹³C NMR (125 MHz, CDCl₃) δ_C = 167.1 (C=C(CN)₂), 164.7 (CO₂Me), 154.7 (C=C(CN)₂), 154.2 (C₅'), 146.7 (DCNQ), 144.9 (C_{8a}'), 143.7 (C_{3a}'), 143.5 (C₂'), 142.9 (C₆'), 142.6 (C_{4',8'}'), 141.5 (C₆'), 140.8 (C_{3a',8a'}'), 140.2 (C₂'), 140.1 (C₄'), 136.6 (C₈'), 136.1 (DCNQ), 134.4 (DCNQ), 132.1 (DCNQ), 131.0 (C₇'), 125.8 (C_{5',7'}'), 125.4 (DCNQ), 124.7 (DCNQ), 124.4 (C₁'), 119.6 (C_{1',3'}'), 118.8 (C₃'), 114.3 (CN), 114.2 (CN), 113.9 (CN), 112.9 (CN), 84.8 (C(CN)₂), 73.7 (C(CN)₂), 51.5 (CO₂Me), 39.4 (*i*Pr), 24.5 (*i*Pr) ppm; HRMS (ESI–TOF, positive) Calcd for C₃₉H₂₆N₄O₂ + Na⁺ [M + Na]⁺ 605.1948, found 605.1948. Anal. Calcd for C₃₉H₂₆N₄O₂·3/4H₂O: C, 78.57; H, 4.65; N, 9.40. Found: C, 78.62; H, 4.51; N, 9.26.

Compound (24). The procedure used for the preparation of 22 was adopted here. The reaction of 10 (131 mg, 0.25 mmol) with TCNE (102 mg, 0.50 mmol) in ethyl acetate (5 mL) at refluxing temperature for 16 h afforded 24 (161 mg, 89%) as dark green crystals: mp 168.0–169.0 °C (CH₂Cl₂/hexane); IR (KBr disk) ν_{max} = 2206 (C≡N), 1700 (C=O) cm⁻¹; UV–vis (CH₂Cl₂) λ_{max} (log ε) = 303 (4.77), 331 sh (4.56), 362 (4.46), 450 sh (4.27), 721 (4.22) nm; UV–vis (10% CH₂Cl₂/hexane) λ_{max} (log ε) = 300 (4.77), 328 sh (4.57), 362 sh (4.44), 448 sh (4.28), 670 (4.13) nm; ¹H NMR (500 MHz, CDCl₃) δ_H = 9.80 (br s, 2H, H₄, H₄ or H₈'), 9.40 (br s, 1H, H₄ or H₈'), 8.62 (s, 1H, H₂'), 8.05 (t, 1H, *J* = 10.0 Hz, H₆'), 7.86 (t, 2H, *J* = 10.0 Hz, H_{5',7'}'), 7.81–7.61 (m, 3H, *J* = 10.0 Hz, H₆ and DCNQ), 7.45 (dd, 1H, *J* = 10.0, 10.0 Hz, H₇'), 7.14 (br s, 1H, DCNQ), 6.98 (dd, 1H, *J* = 9.5, 2.0 Hz, DCNQ), 6.57 (dd, 1H, *J* = 9.5, 2.0 Hz, DCNQ), 4.61 (br s, 2H, CO₂Et), 4.28 (br s, 2H, CO₂Et), 3.92 (s, 3H, CO₂Me), 3.24 (sept, 1H, *J* = 7.0 Hz, *i*Pr), 1.54 (br s, 3H, CO₂Et), 1.42 (d, 6H, *J* = 7.0 Hz, *i*Pr), 1.30 (br s, 3H, CO₂Et) ppm; ¹³C NMR (125 MHz, CDCl₃) δ_C = 167.6 (CO₂Et), 165.1 (CO₂Me), 163.8 (CO₂Et), 153.6 (C₅'), 153.5 (C=C(CN)₂), 147.5 (C=C(CN)₂), 145.7 (DCNQ), 145.3 (C₂'), 144.8 (C_{3a}'), 144.1 (C_{3a',8a'}'), 143.2 (C₆'), 142.2 (C_{4' or C₈'}'), 141.6 (C_{4' or C₈'}'), 140.5 (C₆'), 139.6 (C₄'), 138.0 (DCNQ), 137.7 (DCNQ), 135.8 (C_{5',7'}'), 135.2 (DCNQ), 131.6 (C_{1' or C₃'}'), 131.3 (C_{1' or C₃'}'), 130.0 (C₇'), 125.7 (DCNQ), 125.0 (DCNQ), 118.1 (C₁ or C₃'), 117.5 (C₁ or C₃'), 114.2 (CN), 114.1 (CN), 113.7 (CN), 112.3 (CN), 93.2 (C(CN)₂), 75.6 (C(CN)₂), 61.6 (CO₂Et), 51.4 (CO₂Me), 39.3 (*i*Pr), 24.5 (*i*Pr), 14.5 (CO₂Et) ppm; Three signals (C₈, C_{8a} and C₂') are overlapped with other signals. HRMS (ESI–TOF, positive) Calcd for C₄₅H₃₄N₄O₆ + Na⁺ [M + Na]⁺ 749.2371, found 749.2371. Anal. Calcd for C₄₅H₃₄N₄O₆: C, 74.37; H, 4.72; N, 7.71. Found: C, 74.11; H, 4.62; N, 7.64.

Compound (25). The procedure used for the preparation of 22 was adopted here. The reaction of 12 (131 mg, 0.25 mmol) with TCNQ (102 mg, 0.50 mmol) in ethyl acetate (5 mL) at refluxing temperature for 24 h afforded 26 (145 mg, 80%) as dark green crystals: mp 220.0–222.0 °C (AcOEt); IR (KBr disk) ν_{max} = 2221 (C≡N), 1697 (C=O) cm⁻¹; UV–vis (CH₂Cl₂) λ_{max} (log ε) = 296 sh (4.64), 315 (4.69), 333 sh (4.67), 380 sh (4.48), 461 (4.20), 647 (4.25) nm; UV–vis (10% CH₂Cl₂/hexane) λ_{max} (log ε) = 297 sh (4.65), 310 sh (4.67), 328 sh (4.67), 377 sh (4.47), 446 sh (4.20), 597 (4.24) nm; ¹H NMR (500 MHz, CDCl₃) δ_H = 9.85 (d, 1H, *J* = 1.5 Hz, H₄'), 9.71 (d, 2H, *J* = 11.0 Hz, H_{4',8'}'), 8.90 (s, 1H, H₂'), 8.24 (s, 1H, H₂'), 8.19 (d, 1H, *J* = 10.0 Hz, H₈'), 7.98 (d, 1H, *J* = 10.0 Hz, H₆'), 7.76 (d, 2H, *J* = 11.0 Hz, H_{5',7'}'), 7.66 (dd, 1H, *J* = 10.0, 10.0 Hz, H₇'), 7.34–7.28 (m, 2H, DCNQ), 7.23 (dd, 1H, *J* = 9.5, 1.5 Hz, DCNQ), 7.05

(dd, 1H, $J = 9.5, 1.5$ Hz, DCNQ), 4.41 (q, 4H, $J = 7.0$ Hz, CO₂Et), 3.96 (s, 3H, CO₂Me), 3.27 (sept, 1H, $J = 7.0$ Hz, *i*Pr), 1.44–1.41 (m, 12H, *i*Pr and CO₂Et) ppm; ¹³C NMR (125 MHz, CDCl₃) $\delta_C = 173.9$ (C₆), 164.5 (CO₂Me), 164.2 (CO₂Et), 155.0 (C₅), 153.3 (C=C(CN)₂), 146.8 (C₂), 145.5 (C=C(CN)₂), 144.6 (DCNQ), 143.8 (C_{3a} or C_{8a} or C_{3a',8a'}), 143.7 (C_{3a} or C_{8a} or C_{3a',8a'}), 143.3 (C₂), 141.7 (C₆), 140.5 (C₄), 137.9 (C_{4',8'}), 136.2 (DCNQ), 135.8 (C₈), 135.5 (DCNQ), 133.2 (DCNQ), 130.9 (C₇), 129.5 (C_{5',7'}), 126.7 (DCNQ), 126.6 (DCNQ), 123.2 (C₁), 118.9 (C₃), 118.6 (C_{1',3'}), 113.8 (CN), 113.7 (CN), 112.1 (CN), 111.7 (CN), 91.6 (C(CN)₂), 60.6 (CO₂Et), 51.7 (CO₂Me), 39.4 (*i*Pr), 24.5 (*i*Pr), 14.5 (CO₂Et) ppm; Two signals are overlapped with other signals. HRMS (ESI–TOF, positive) Calcd for C₄₅H₃₄N₄O₆ + Na⁺ [M + Na]⁺ 749.2371, found 749.2371. Anal. Calcd for C₄₅H₃₄N₄O₆·2/3H₂O: C, 73.16; H, 4.82; N, 7.58. Found: C, 73.23; H, 4.90; N, 7.69.

Compound (26). The procedure used for the preparation of **22** was adopted here. The reaction of **13** (134 mg, 0.25 mmol) with TCNQ (102 mg, 0.50 mmol) in ethyl acetate (5 mL) at refluxing temperature for 23 h afforded **27** (158 mg, 85%) as dark green crystals: mp 195.0–197.0 °C (CH₂Cl₂/hexane); IR (KBr disk) $\nu_{\max} = 2208$ (C≡N), 1681 (C=O) cm⁻¹; UV–vis (CH₂Cl₂) λ_{\max} (log ϵ) = 246 (4.76), 299 (4.62), 347 (4.70), 448 (4.49), 644 (4.37) nm; UV–vis (10% CH₂Cl₂/hexane) λ_{\max} (log ϵ) = 244 (4.75), 299 (4.62), 346 (4.69), 445 (4.48), 586 (4.37) nm; ¹H NMR (500 MHz, CDCl₃) $\delta_H = 9.88$ (d, 1H, $J = 1.5$ Hz, H₄), 8.98 (d, 2H, $J = 11.5$ Hz, H_{4',8'}), 8.26 (d, 1H, $J = 10.0$ Hz, H₈), 8.25 (s, 1H, H₂), 8.18 (s, 2H, NH₂), 7.99 (d, 1H, $J = 10.0$ Hz, H₆), 7.68 (d, 2H, $J = 11.5$ Hz, H_{5',7'}), 7.67 (dd, 1H, $J = 10.0, 10.0$ Hz, H₇), 7.23–7.17 (m, 3H, DCNQ), 7.08 (dd, 1H, $J = 9.5, 2.0$ Hz, DCNQ), 4.46 (q, 4H, $J = 7.0$ Hz, CO₂Et), 3.96 (s, 3H, CO₂Me), 3.29 (sept, 1H, $J = 7.0$ Hz, *i*Pr), 1.47–1.44 (m, 12H, *i*Pr and CO₂Et) ppm; ¹³C NMR (125 MHz, CDCl₃) $\delta_C = 174.9$ (C₆), 165.8 (CO₂Et), 164.6 (CO₂Me), 155.0 (C₅), 153.5 (C=C(CN)₂), 146.7 (C_{3a',8a'}), 145.5 (C=C(CN)₂), 144.8 (DCNQ), 143.9 (C₂), 143.6 (C_{3a}), 141.7 (C₆), 140.3 (C₄), 137.2 (C_{1',3'}), 136.4 (DCNQ), 136.1 (C₈), 134.9 (DCNQ), 133.7 (DCNQ), 132.6 (C_{5',7'}), 131.0 (C₇), 128.5 (C_{4',8'}), 126.1 (DCNQ), 125.8 (DCNQ), 124.7 (C₁), 119.0 (C₃), 114.0 (CN), 113.9 (CN), 113.1 (CN), 112.4 (CN), 102.4 (C₂), 88.1 (C(CN)₂), 75.5 (C(CN)₂), 60.6 (CO₂Et), 51.6 (CO₂Me), 39.4 (*i*Pr), 24.5 (*i*Pr), 14.6 (CO₂Et) ppm; One signal is overlapped with other signal. HRMS (ESI–TOF, positive) Calcd for C₄₅H₃₅N₅O₆ + Na⁺ [M + Na]⁺ 764.2480, found 764.2480. Anal. Calcd for C₄₅H₃₅N₅O₆·H₂O: C, 71.13; H, 4.91; N, 9.22. Found: C, 71.07; H, 4.95; N, 9.20.

■ ASSOCIATED CONTENT

Ⓢ Supporting Information

Copies of ¹H and ¹³C NMR spectra and COSY, UV–vis spectra, and continuous change in the visible spectra, cyclic and differential pulse voltammograms of the reported compounds. This material is available free of charge via the Internet at <http://pubs.acs.org>.

■ AUTHOR INFORMATION

Corresponding Author

*E-mail: tshoji@shinshu-u.ac.jp.

Notes

The authors declare no competing financial interest.

■ ACKNOWLEDGMENTS

This work was partially supported by a Grant-in-Aid for Research (No. 22850007 and 25810019 to T.S.) from the Ministry of Education, Culture, Sports, Science, and Technology, Japan.

■ REFERENCES

(1) (a) Brédas, J. L.; Adant, C.; Tackx, P.; Persoons, A.; Pierce, B. M. *Chem. Rev.* **1994**, *94*, 243–278. (b) Bendikov, M.; Wudl, F.;

Perepichka, D. F. *Chem. Rev.* **2004**, *104*, 4891–4945. (c) Hünig, S.; Herberth, E. *Chem. Rev.* **2004**, *104*, 5535–5564. (d) Baumgartner, T.; Réau, R. *Chem. Rev.* **2006**, *106*, 4681–4727. (e) Clavier, G.; Audebert, P. *Chem. Rev.* **2010**, *110*, 3299–3314.

(2) (a) Kivala, M.; Stanoeva, T.; Michinobu, T.; Frank, B.; Gescheidt, G.; Diederich, F. *Chem.—Eur. J.* **2008**, *14*, 7638–7647. (b) Esembeson, B.; Scimeca, M. L.; Michinobu, T.; Diederich, F.; Biaggio, I. *Adv. Mater.* **2008**, *20*, 4584–4587. (c) Frank, B. B.; Blanco, B. C.; Jakob, S.; Ferroni, F.; Pieraccini, S.; Ferrarini, A.; Boudon, C.; Gisselbrecht, J.-P.; Seiler, P.; Spada, G. P.; Diederich, F. *Chem.—Eur. J.* **2009**, *15*, 9005–9016. (d) Koos, C.; Vorreau, P.; Vallaitis, T.; Dumon, P.; Bogaerts, W.; Baets, R.; Esembeson, B.; Biaggio, I.; Michinobu, T.; Diederich, F.; Freude, W.; Leuthold, J. *Nat. Photonics* **2009**, *3*, 216–219. (e) Frank, B. B.; Kivala, M.; Blanco, B. C.; Breiten, B.; Schweizer, W. B.; Laporta, P. R.; Biaggio, I.; Jahnke, E.; Tykwinski, R. R.; Boudon, C.; Gisselbrecht, J.-P.; Diederich, F. *Eur. J. Org. Chem.* **2010**, 2487–2503. (f) Breiten, B.; Wu, Y.-L.; Jarowski, P. D.; Gisselbrecht, J.-P.; Boudon, C.; Griesser, M.; Onitsch, C.; Gescheidt, G.; Schweizer, W. B.; Langer, N.; Lennartz, C.; Diederich, F. *Chem. Sci.* **2011**, *2*, 88–93. (g) Lacy, A. R.; Vogt, A.; Boudon, C.; Gisselbrecht, J.-P.; Schweizer, W. B.; Diederich, F. *Eur. J. Org. Chem.* **2013**, 869–879. (h) Tchitchanov, B. H.; Chiu, M.; Jordan, M.; Kivala, M.; Schweizer, W. B.; Diederich, F. *Eur. J. Org. Chem.* **2013**, 3729–3740. (i) Fujita, H.; Tsuboi, K.; Michinobu, T. *Macromol. Chem. Phys.* **2011**, *212*, 1758–1766. (j) Li, Y.; Ashizawa, M.; Uchida, S.; Michinobu, T. *Macromol. Rapid Commun.* **2011**, *32*, 1804–1808. (k) Michinobu, T.; Seo, C.; Noguchi, K.; Mori, T. *Polym. Chem.* **2012**, *3*, 1427–1435. (l) Li, Y.; Ashizawa, M.; Uchida, S.; Michinobu, T. *Polym. Chem.* **2012**, *3*, 1996–2005.

(3) (a) Kivala, M.; Boudon, C.; Gisselbrecht, J.-P.; Seiler, P.; Gross, M.; Diederich, F. *Chem. Commun.* **2007**, 4731–4733. (b) Kivala, M.; Boudon, C.; Gisselbrecht, J.-P.; Enko, B.; Seiler, P.; Müller, I. B.; Langer, N.; Jarowski, P. D.; Gescheidt, G.; Diederich, F. *Chem.—Eur. J.* **2009**, *15*, 4111–4123. (c) Kato, S.; Kivala, M.; Schweizer, W. B.; Boudon, C.; Gisselbrecht, J.-P.; Diederich, F. *Chem.—Eur. J.* **2009**, *15*, 8687–8691. (d) Fesser, P.; Iacovita, C.; Wäckerlin, C.; Vijayaraghavan, S.; Ballav, N.; Howes, K.; Gisselbrecht, J.-P.; Crobu, M.; Boudon, C.; Stöhr, M.; Jung, T. A.; Diederich, F. *Chem.—Eur. J.* **2011**, *17*, 5246–5250. (e) Yuan, Y.; Michinobu, T. *J. Polym. Sci., Part A: Polym. Chem.* **2011**, *49*, 225–233. (f) Washino, Y.; Michinobu, T. *Macromol. Rapid Commun.* **2011**, *32*, 644–648.

(4) (a) Jarowski, P. D.; Wu, Y.-L.; Boudon, C.; Gisselbrecht, J.-P.; Gross, M.; Schweizer, W. B.; Diederich, F. *Org. Biomol. Chem.* **2009**, *7*, 1312–1322. (b) Silvestri, F.; Jordan, M.; Howes, K.; Kivala, M.; Rivera-Fuentes, P.; Boudon, C.; Gisselbrecht, J.-P.; Schweizer, W. B.; Seiler, P.; Chiu, M.; Diederich, F. *Chem.—Eur. J.* **2011**, *17*, 6088–6097. (c) Tancini, F.; Wu, Y.-L.; Schweizer, W. B.; Gisselbrecht, J.-P.; Boudon, C.; Jarowski, P. D.; Beels, M. T.; Biaggio, I.; Diederich, F. *Eur. J. Org. Chem.* **2012**, 2756–2765.

(5) Zeller, K.-P. *Azulene*. In *Methoden der Organischen Chemie* (Houben-Weyl), 4th ed.; Kropf, H., Ed.; Thieme: Stuttgart, 1985; Vol. V, Part 2c, pp 127–418.

(6) (a) Ito, S.; Inabe, H.; Okujima, T.; Morita, N.; Watanabe, M.; Harada, N.; Imafuku, K. *J. Org. Chem.* **2001**, *66*, 7090–7101. (b) Ito, S.; Okujima, T.; Morita, N. *J. Chem. Soc. Perkin Trans. 1* **2002**, 1896–1905. (c) Ito, S.; Inabe, H.; Morita, N.; Ohta, K.; Kitamura, T.; Imafuku, K. *J. Am. Chem. Soc.* **2003**, *125*, 1669–1680. (d) Ito, S.; Kubo, T.; Morita, N.; Ikoma, T.; Tero-Kubota, S.; Tajiri, A. *J. Org. Chem.* **2003**, *68*, 9753–9762. (e) Ito, S.; Inabe, H.; Morita, N.; Tajiri, A. *Eur. J. Org. Chem.* **2004**, 1774–1780. (f) Ito, S.; Kubo, T.; Morita, N.; Ikoma, T.; Tero-Kubota, S.; Kawakami, J.; Tajiri, A. *J. Org. Chem.* **2005**, *70*, 2285–2293. (g) Ito, S.; Iida, T.; Kawakami, J.; Okujima, T.; Morita, N. *Eur. J. Org. Chem.* **2009**, 5355–5364. (h) Shoji, T.; Shimomura, E.; Maruyama, M.; Ito, S.; Okujima, T.; Morita, N. *Eur. J. Org. Chem.* **2013**, 957–964.

(7) (a) Shoji, T.; Ito, S.; Toyota, K.; Yasunami, M.; Morita, N. *Chem.—Eur. J.* **2008**, *14*, 8398–8408. (b) Shoji, T.; Ito, S.; Toyota, K.; Iwamoto, T.; Yasunami, M.; Morita, N. *Eur. J. Org. Chem.* **2009**, 4316–4324. (c) Shoji, T.; Maruyama, M.; Ito, S.; Morita, N. *Bull. Chem. Soc.*

- Jpn. 2012*, *85*, 761–773. (d) Shoji, T.; Ito, S.; Okujima, T.; Morita, N. *Org. Biomol. Chem.* **2012**, *10*, 8308–8313. (e) Shoji, T.; Ito, S.; Okujima, T.; Morita, N. *Chem.—Eur. J.* **2013**, *19*, 5721–5730.
- (8) Ito, S.; Nomura, A.; Morita, N.; Kabuto, C.; Kobayashi, H.; Maejima, S.; Fujimori, K.; Yasunami, M. *J. Org. Chem.* **2002**, *67*, 7295–7302.
- (9) Nozoe, T.; Seto, S.; Matsumura, S. *Bull. Chem. Soc. Jpn.* **1962**, *35*, 1990–1998.
- (10) Corbet, J.-P.; Mignani, G. *Chem. Rev.* **2006**, *106*, 2651–2710.
- (11) McDonald, R. N.; Richmond, J. M.; Curtis, J. R.; Petty, H. E.; Hoskins, T. L. *J. Org. Chem.* **1976**, *41*, 1811–1821.
- (12) Nozoe, T.; Seto, S.; Matsumura, S.; Murase, Y. *Bull. Chem. Soc. Jpn.* **1962**, *35*, 1179–1188.
- (13) Elwahi, A. H. M.; Hafner, K. *Tetrahedron Lett.* **2000**, *41*, 2859–2862.
- (14) Ito, S.; Inabe, H.; Okujima, T.; Morita, N.; Watanabe, M.; Imafuku, K. *Tetrahedron Lett.* **2000**, *41*, 8343–8347.
- (15) Reutenauer, P.; Kivala, M.; Jarowski, P. D.; Boudon, C.; Gisselbrecht, J.; Gross, M.; Diederich, F. *Chem. Commun.* **2007**, 4898–4900.
- (16) Silverstein, R. M.; Webster, F. X.; Kiemle, D. *Spectrometric Identification of Organic Compounds*, 7th ed.; John Wiley and Sons: Weinheim, Germany, 2005.
- (17) The B3LYP/6-31G** time-dependence density functional calculations were performed with Spartan'10, Wavefunction, Irvine, CA.
- (18) (a) Suppan, P.; Ghoneim, N. *Solvatochromism*; The Royal Society of Chemistry: Cambridge, 1997. (b) Christian, R. *Solvent and Solvent Effects in Organic Chemistry*; Wiley-VCH: Weinheim, Germany, 2004.
- (19) (a) Ito, S.; Morita, N. *Eur. J. Org. Chem.* **2009**, 4567–4579. (b) Ito, S.; Shoji, T.; Morita, N. *Synlett* **2011**, 2279–2298. (c) Shoji, T.; Higashi, J.; Ito, S.; Okujima, T.; Yasunami, M.; Morita, N. *Chem.—Eur. J.* **2011**, *17*, 5116–5129. (d) Shoji, T.; Higashi, J.; Ito, S.; Okujima, T.; Yasunami, M.; Morita, N. *Org. Biomol. Chem.* **2012**, *10*, 2431–2438.